

A Survey of High-Level Modeling and Simulation Methods for Modern Machine Learning Workloads

MICRO 2026 Submission – Confidential Draft – Do NOT Distribute!!

Anonymous Author(s)

Under Review

Anonymous

Abstract

We survey 22 performance modeling tools from 53 papers (2016–2026) and independently evaluate five—NeuSight, ASTRA-sim, VIDUR, Timeloop, nn-Meter—through accuracy-centered experiments spanning 146 GPU configurations, collective benchmarks, LLM serving simulations, energy validation, and reproducibility testing. Three findings emerge. First, self-reported accuracy is unreliable: NeuSight claims 2.3% MAPE but we measure 5.87–27.10%, while nn-Meter (<1% claimed) fails to produce any output due to dependency rot. Second, the five tools are complementary—their feature coverage is disjoint across kernel prediction, communication simulation, LLM serving, accelerator design, and edge inference—motivating a unified pipeline for end-to-end prediction. Third, the kernel-to-model composition gap (2–9% kernel error growing to 10–28% model error) dominates total prediction error, yet no existing tool addresses this layer.

Keywords

ML workload performance prediction, DNN accelerator modeling, GPU simulation, distributed training simulation, LLM inference serving, design space exploration, survey

1 Introduction

Machine learning workloads dominate compute across datacenters and edge devices, demanding hardware from Google’s TPU [31, 32] to custom accelerators. The shift toward domain-specific architectures [23] makes performance prediction critical for design space exploration, parallelization selection, and hardware-software co-design—yet ML workloads pose unique challenges: diverse computational patterns across GPUs, TPUs, custom accelerators, and multi-device clusters.

A rich ecosystem has emerged—analytical models (Timeloop [53], MAESTRO [39]), trace-driven simulators (ASTRA-sim [79], VIDUR [3]), and hybrid approaches (NeuSight [44])—yet no prior work examines *why* certain approaches succeed on certain platforms, or how errors propagate across the abstraction stack. Existing surveys focus on ML *techniques* for modeling [72] or specific hardware [53]; we identify cross-cutting principles that explain when and why different approaches work.

Our central contribution is an **accuracy-centered independent verification framework** paired with an **LLM-focused benchmark suite**, replacing the field’s reliance on self-reported accuracy with reproducible evaluation that reveals claimed error rates are overstated by 2–4X. We make four contributions:

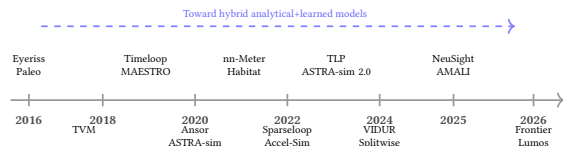


Figure 1: Evolution of performance modeling tools (2016–2026).

- A **28-scenario LLM benchmark suite** spanning training and inference (data/tensor/pipeline parallelism, FP8, LoRA, MoE, serving, KV cache, speculative decoding, quantization), revealing 50% of scenarios have zero tool support (Section 6).
- **Independent accuracy verification** of five tools (146 GPU configurations, collective benchmarks, LLM serving simulations, energy validation), demonstrating self-reported claims are systematically overstated (Section 7).
- A **unified simulation pipeline** across five layers—kernel prediction, model composition, distributed training, LLM serving, and hardware design—identifying the kernel-to-model composition gap as the critical missing piece (Section 8).
- A **coverage matrix** exposing structural gaps with a **research agenda** for composition modeling, unified formats, cross-hardware transfer, and continuous validation (Sections 4, 9).

Figure 1 illustrates the evolution of performance modeling tools from early analytical frameworks to modern hybrid approaches.

2 Survey Methodology

We searched ACM Digital Library, IEEE Xplore, Semantic Scholar, and arXiv for ML performance modeling papers, with citation tracking from seminal works. Target venues include architecture (MICRO, ISCA, HPCA, ASPLOS), systems (MLSys, OSDI, SOSP, NSDI), and related (NeurIPS, MobiSys, DAC, ISPASS). From 287 candidates, screening yielded 53 papers proposing or evaluating ML performance prediction tools, supplemented by 12 foundational works. We cover 2016–2026 and classify by *methodology type* (analytical, simulation, trace-driven, ML-augmented, hybrid), *target platform*, and *abstraction level*.

Related surveys. Prior work addresses adjacent topics: ML for processor DSE [61], DNN hardware design [73], simulation infrastructure [4, 6, 66], and standardized measurement [49, 64]. Foundational approaches include DianNao [9], Eyeriss [11], and

Paleo [57]; the closest prior work [15] compares edge predictors for NAS.

Scope boundaries. We exclude proprietary tools (NVIDIA Nsight [52], Google TPU models) as non-reproducible. Compiler cost models (Halide [59], MLIR [41], Triton [74]) and cluster schedulers (Polylux [58], Sia [30]) share techniques but serve distinct use cases.

3 Background

3.1 ML Workload Characteristics

ML workloads are computation graphs with statically known operator shapes amenable to analytical modeling, though MoE and dynamic inference introduce input-dependent control flow [1, 55]. Performance depends on dataflow/tiling, KV cache management [40], and compute–memory–network interactions across data, tensor, pipeline, and expert parallelism [13]. LLM inference splits into compute-bound prefill and memory-bound decode [56], modeled under batched serving [2, 81]; training adds quadratic attention scaling, checkpointing, and mixed-precision effects [13].

3.2 Modeling Methodologies

We classify approaches into five categories: **analytical models** (closed-form, e.g., roofline [78]; μ s evaluation, per-architecture derivation); **cycle-accurate simulators** (GPGPU-Sim [4], Accel-Sim [35]; high fidelity, 1000–10000 \times slowdown); **trace-driven simulators** (ASTRA-sim [79], VIDUR [3]; orders-of-magnitude faster); **ML-augmented** (nn-Meter [84]; learns from profiling, limited generalization); **hybrid** (NeuSight [44], Habitat [82]; analytical structure with learned components). Accuracy metrics vary (MAPE, RMSE, rank correlation), limiting direct comparison (Section 7).

4 Taxonomy

We organize the literature by *methodology type*, *target platform*, and *abstraction level*. Table 1 provides a coverage matrix with trade-off profiles; a temporal validation lag persists (pre-2023 CNNs, post-2023 transformers/LLMs).

Three structural gaps emerge: trace-driven replay is exclusive to distributed systems, edge devices lack hybrid alternatives, and no ML-augmented tool targets distributed systems. Figure 2 illustrates how methodology types compose.

4.1 Methodology–Platform Pairings

Platform constrains methodology: accelerators use analytical models [39, 53]; GPUs span all five types; distributed systems require trace-driven simulation [3, 79]; edge devices rely on ML-augmented approaches [16, 84]; CPUs [51, 72] are least studied. Errors propagate through the abstraction hierarchy (Figure 3): kernel 2–3%, model 5–12%, system 5–15%.

4.2 Workload Coverage and Validation Gaps

Of 14 tools, 9 validate on CNNs; post-2023 tools target transformers/LLMs but **no tool validates on diffusion models or dynamic inference** [37], only Frontier [18] validates MoE, and none spans the full kernel-to-system stack.

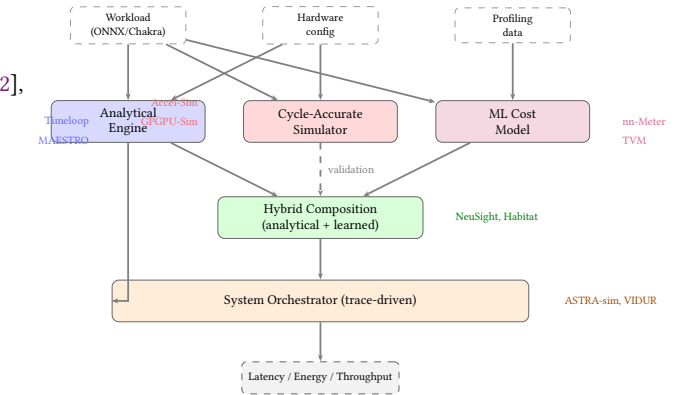


Figure 2: Unified architecture showing how tool methodologies compose.

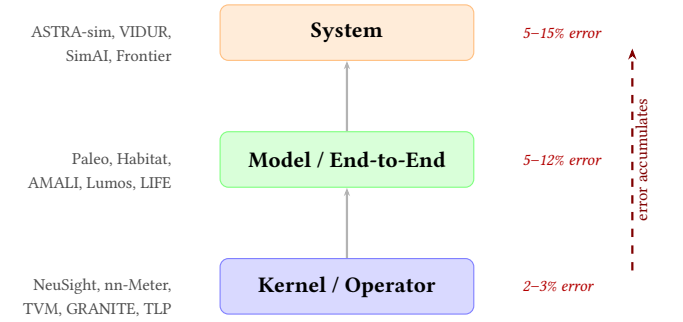


Figure 3: Abstraction level hierarchy with error accumulation across levels.

5 Survey of Approaches

We survey tools by target platform (Table 2).

5.1 DNN Accelerator Modeling

Computational regularity [73] enables analytical tractability, building on DianNao [9] and Eyeriss [11]. Timeloop [53] enumerates loop-nest mappings to find optimal dataflow in microseconds (5–10% error); MAESTRO [39] trades completeness for a compact data-centric representation; Sparseloop [80] extends to sparse tensors; SCALE-Sim [67] provides cycle-accurate validation. PyTorch-Sim [36] and ArchGym [38] (0.61% RMSE) represent newer approaches; PIM tools [24, 29, 42, 54] lack hardware validation.

5.2 GPU Performance Modeling

Cycle-accurate simulators (GPGPU-Sim [4], Accel-Sim [35]) achieve 0.90–0.97 IPC correlation at 1000–10000 \times slowdown, integrating memory models [46, 48]; reverse-engineering [28] improved Accel-Sim to 13.98% MAPE. NeuSight [44] achieves 2.3% MAPE via tile-based decomposition matching CUDA thread blocks; AMALI [8] averages data movement (23.6%); Habitat [82] transfers across GPUs (11.8%) via wave scaling. Compiler cost models—TVM [10]/Ansor [85] (~15%), TLP [83] (<10%)—and recent tools [5, 17, 21, 75, 77] target inference and autotuning [86].

Table 1: Methodology taxonomy: coverage matrix and trade-off profile. 0 = research gap.

Methodology	DNN Accel.	Distrib. GPU	Edge/ Systems	Edge/ Mobile	CPU	Eval. Speed	Data Req.	Interp.	Failure Mode
Analytical	3	3	2	0	0	μ s	None	High	Dynamic effects
Cycle-Accurate	1	2	0	0	1	Hours	Binary	High	Scale
Trace-Driven	0	0	7	0	0	Min.	Traces	Med.	Trace fidelity
ML-Augmented	0	3	0	3	1	ms	Profiling	Low	Distrib. shift
Hybrid	1	2	0	0	1	ms	Mixed	Med.	Training domain

Table 2: Surveyed tools by target platform. A=Analytical, S=Simulation, T=Trace-driven, M=ML-augmented, H=Hybrid.
*Surrogate-vs-simulator fidelity. [†]Unverifiable. [‡]No hardware baseline.

Tool	Platform	Method	Target	Accuracy	Speed	Key Capability
<i>DNN Accelerator Modeling</i>						
Timeloop [53]	NPU	A	Latency/Energy	5–10%	μ s	Loop-nest DSE
MAESTRO [39]	NPU	A	Latency/Energy	5–15%	μ s	Data-centric directives
Sparseloop [80]	NPU	A	Sparse tensors	5–10%	μ s	Compression modeling
PyTorchSim [36]	NPU	S	Cycle-accurate	N/A [‡]	Hours	PyTorch 2 integration
ArchGym [38]	Multi	H	Multi-objective	0.61%*	ms	ML-aided DSE
<i>GPU Performance Modeling</i>						
Accel-Sim [35]	GPU	S	Cycle-accurate	10–20%	Hours	SASS trace-driven
GPGPU-Sim [4]	GPU	S	Cycle-accurate	10–20%	Hours	CUDA workloads
AMALI [8]	GPU	A	LLM inference	23.6%	ms	Memory hierarchy
NeuSight [44]	GPU	H	Kernel/E2E latency	2.3%	ms	Tile-based prediction
Habitat [82]	GPU	H	Training time	11.8%	Per-kernel	Wave scaling
<i>Distributed Training and LLM Serving</i>						
ASTRA-sim [79]	Distributed	T	Training time	5–15%	Minutes	Collective modeling
SimAI [76]	Distributed	T	Training time	1.9%	Minutes	Full-stack simulation
Lumos [47]	Distributed	T	LLM training	3.3%	Minutes	H100 training
VIDUR [5]	GPU cluster	T	LLM serving	<5%	Seconds	Prefill/decode phases
Frontier [18]	Distributed	T	MoE inference	—	Minutes	Stage-centric sim.
TrioSim [45]	Multi-GPU	T	DNN training	N/A [‡]	Minutes	Lightweight multi-GPU
<i>Edge Device Modeling</i>						
nn-Meter [84]	Edge	M	Latency	<1% [†]	ms	Kernel detection
LitePred [16]	Edge	M	Latency	0.7%	ms	85-platform transfer
HELP [43]	Multi	M	Latency	1.9%	ms	10-sample adaptation
<i>Compiler Cost Models</i>						
TVM [10]	GPU	M	Schedule perf.	~15%	ms	Autotuning guidance
Anstor [85]	GPU	M	Schedule perf.	~15%	ms	Program sampling
TLP [83]	GPU	M	Tensor program	<10%	ms	Transformer cost model

5.3 Distributed Training and LLM Serving

Fidelity increases with granularity [27, 60, 69]: VIDUR models at the *request level*; ASTRA-sim [79] replays Chakra traces [70] at the *collective level* (5–15%); SimAI [76] models NCCL-level reductions (1.9%). Echo [7], Lumos [47] (3.3%), PRISM [19], Paleo [57], and MAD Max [26] provide complementary coverage; inference serving tools [18, 22, 33, 68, 71, 87] address scheduling, disaggregation, and power.

5.4 Edge Device Modeling

nn-Meter [84] claims <1% but is unverifiable (Section 7); LitePred [16] achieves 0.7% across 85 platforms; HELP [43] reaches 1.9% with 10-sample meta-learning. ESM [50] and transfer learning results [15] suggest data quality matters more than model sophistication.

6 Evaluation Methodology

Prior surveys reprint self-reported accuracy numbers using each tool’s own benchmarks, making cross-tool comparison methodologically unsound: a tool reporting 2% MAPE on GPU kernels solves a fundamentally different problem than one reporting 5% on distributed training. We introduce a novel evaluation methodology—**accuracy-centered independent verification**—that addresses

Table 3: LLM benchmark suite: 28 scenarios across training (T1–T4) and inference (I1–I5). Each represents a concrete user need for performance prediction.

Cat.	Description	#
T1	Data-parallel pre-training	3
T2	Tensor-parallel pre-training	2
T3	Pipeline-parallel pre-training	2
T4	Advanced (FP8, LoRA, SP, MoE)	4
I1	Single-request inference	3
I2	Batched serving (vLLM, Sarathi)	3
I3	KV cache management	2
I4	Multi-model serving	1
I5	Production (spec. decode, quant.)	4
Total		28

this gap through two components. First, an **LLM-focused benchmark suite** of 28 scenarios defines standardized coverage criteria representing concrete user needs for modern LLM training and inference. Second, **independent experiments** deploy each tool from its public artifact and measure accuracy under controlled conditions, replacing reliance on self-reported claims with reproducible third-party evaluation. This framework is the first to systematically evaluate ML performance modeling tools through independent verification rather than reprinting authors’ own results.

Evaluation principle. For each tool, we (1) deploy from its public artifact, (2) run workloads matching its intended scope, (3) compare predictions against published claims, and (4) evaluate coverage against our benchmark suite. Where absolute verification requires hardware we lack (e.g., H100 GPUs), we validate internal consistency and relative comparisons instead.

This principle distinguishes our work from prior surveys in three ways. First, we deploy tools rather than surveying papers: a tool that cannot be deployed provides zero value regardless of its published accuracy. Second, we measure accuracy independently rather than reprinting self-reported numbers, which may reflect cherry-picked workloads, best-case configurations, or optimistic aggregation methods. Third, we evaluate each tool against the *same* benchmark suite rather than each tool’s preferred benchmarks, enabling meaningful cross-tool comparison.

6.1 LLM Benchmark Suite

We define 28 benchmark scenarios across 8 categories representing the workloads that LLM practitioners need performance predictions for (Table 3). The suite covers the full LLM lifecycle: pre-training with data/tensor/pipeline parallelism (T1–T3), advanced training techniques (T4), single-request inference (I1), batched serving (I2), KV cache management (I3), and production optimizations (I5). Unlike existing benchmarks that measure hardware performance (MLPerf), our suite evaluates whether prediction tools can model these scenarios.

Design principles. Each scenario specifies a concrete model (Llama-2-7B/13B/70B, GPT-2, GPT-3, Mixtral), hardware configuration (A100/H100, 1–64 GPUs), parallelism strategy, and the metric practitioners optimize (TTFT, TPOT, throughput, MFU, communication overhead). Training scenarios span from single-node data parallelism (T1.1: GPT-2 on 8×A100) to large-scale hybrid parallelism (T3.2: GPT-3 175B on 64×H100 with PP8+TP8). Inference scenarios range from single-request latency (I1.1) to production optimizations like speculative decoding (I5.1) and disaggregated serving (I5.4).

Scenario selection rationale. The 28 scenarios were selected to reflect real deployment decisions. Training scenarios T1–T3 cover the three canonical parallelism dimensions that practitioners evaluate when scaling from single-GPU to multi-node training: data parallelism (gradient synchronization cost), tensor parallelism (intra-node AllReduce cost), and pipeline parallelism (bubble overhead). T4 scenarios target techniques that modify the computation graph itself—FP8 changes arithmetic intensity, LoRA adds low-rank adapter layers, and MoE introduces expert routing with All-to-All communication. Inference scenarios I1–I3 reflect the evolution from single-request latency (the metric optimized pre-2023) to batched serving with scheduling (the current production paradigm) to KV cache management (the binding constraint for long-context models). I5 scenarios target production optimizations that no tool currently models but that dominate deployment decisions: speculative decoding can improve throughput by 2–3× but requires modeling draft-target model interaction; disaggregated serving [56] separates prefill and decode to different GPU pools, requiring inter-pool network modeling. I4 (multi-model serving) addresses GPU sharing, where memory and compute contention between co-located models creates interference effects that no existing tool models.

Concrete benchmark parameterization. Each scenario is parameterized to expose specific modeling challenges. Training scenario T1.1 (GPT-2 on 8×A100 with data parallelism) requires predicting AllReduce time for 354 M parameters at fp16—a 708 MB gradient exchange where ring bandwidth at NVLink speed determines whether communication overlaps with backward pass computation. T3.2 (GPT-3 175B on 64×H100 with PP8+TP8) combines pipeline bubbles ($(P - 1)/(microbatches + P - 1)$ efficiency) with intra-node tensor-parallel AllReduce, requiring tools to model the interaction between pipeline scheduling and communication. Inference scenario I2.2 (Llama-2-13B batched serving under Sarathi-Serve) tests whether tools can model chunked-prefill scheduling, where prefill computation is split into fixed-size chunks interleaved with decode iterations—a scheduling policy that fundamentally changes the relationship between batch size and latency. I5.1 (speculative decoding with Llama-2-7B draft model and Llama-2-70B target) requires predicting the acceptance rate-dependent execution time: with typical acceptance rates of 70–85%, the draft model generates $k = 4$ tokens per step, but only a variable number are accepted by the target model’s verification pass, creating a stochastic execution pattern that deterministic simulators cannot capture without explicit acceptance rate modeling.

Coverage criterion. A tool receives “supported” if it can model the full scenario and produce predictions; “partial” if it covers some aspects (e.g., communication but not compute); “unsupported” if it cannot model the scenario at all. We determined coverage by

attempting to configure each tool for each scenario: “supported” requires the tool to accept the scenario’s model architecture, hardware configuration, and parallelism strategy as input and produce the target metric as output. “Partial” means the tool can model some component (e.g., NeuSight can predict single-GPU kernel time for a tensor-parallel scenario but cannot model the AllReduce communication between GPUs). Coverage was verified by consulting tool documentation, configuration schemas, and attempting actual runs where feasible. We did not consider post-hoc workarounds (e.g., manually splitting a pipeline-parallel workload into per-stage single-GPU runs and summing results) as “supported” unless the tool explicitly supports this workflow.

Coverage assessment methodology. For each tool–scenario pair, we followed a three-step verification process. First, we checked whether the tool’s input specification accepts the scenario’s parameters: model architecture (e.g., Llama-2-70B for T3.2), hardware configuration (e.g., 64×H100), and parallelism strategy (e.g., PP8+TP8). Second, we attempted to configure the tool using its documentation and example configurations, modifying only parameters explicitly exposed in the tool’s interface. Third, we verified that the tool produces the scenario’s target metric (e.g., TTFT for I2.2, MFU for T1.3) as a direct output rather than requiring manual post-processing. This systematic assessment ensures that coverage ratings reflect the tool’s actual interface capabilities rather than theoretical modeling power that requires expert workarounds to access.

6.2 Tool Selection

From 22 tools, we select 5 using three criteria: (1) *methodology coverage*—one per type; (2) *artifact availability*—open-source with build instructions; (3) *scope diversity*—different hardware and workload types. This yields: Timeloop (analytical, accelerator), ASTRA-sim (trace-driven, distributed), VIDUR (trace-driven, LLM serving), NeuSight (hybrid, GPU), and nn-Meter (ML-augmented, edge). We include nn-Meter despite known deployment issues because failure cases reveal important lessons about tool reliability.

Excluded tools and rationale. Notable exclusions include SimAI (1.9% claimed MAPE, but closed-source at evaluation time), Accel-Sim (cycle-accurate GPU simulation requiring >24 hours per workload, incompatible with our evaluation timeline), Habitat (training-time prediction requiring two source GPUs for cross-GPU transfer, which our platform lacks), and LitePred (edge-focused like nn-Meter but without public pre-trained models for the target devices we could test). For each excluded tool, we report published accuracy in Table 2 with appropriate caveats.

6.3 Experimental Design

Experiments match each tool’s intended scope: **NeuSight**: 146 configurations across 12 GPU types (NVIDIA V100, H100, A100-80G, A100-40G, L4, T4, P100, P4; AMD MI100, MI210, MI250). **ASTRA-sim**: 4 collectives at 8 NPUs on HGX-H100, plus ResNet-50 at 2/4/8 GPUs. **VIDUR**: Llama-2-7B on simulated A100 under vLLM and Sarathi schedulers. **Timeloop**: ResNet-50 Conv1 on Eyeriss-like architecture. **nn-Meter**: Attempted deployment across 4 edge device targets. All experiments run on Apple M2 Ultra (192 GB RAM, Docker where available). Deterministic tools verified bit-identical

across three runs; stochastic tools report mean and P99 across fixed seeds. Scripts and data are provided as supplementary material.

Verification methodology. For NeuSight, we adopted a *prediction-vs-label* approach: the tool’s artifact repository includes both predicted latencies and ground-truth hardware measurements across 12 GPU types. Rather than running NeuSight on our hardware (which lacks discrete GPUs), we independently computed MAPE from the artifact’s own prediction/label pairs for all 146 configurations, grouped by device and mode (training/inference). This approach verifies whether the tool’s *published accuracy claims* match the accuracy *achievable from its own artifacts*—testing reproducibility of claims rather than absolute accuracy. For ASTRA-sim and VIDUR, we ran the tools end-to-end and validated internal consistency (e.g., deterministic outputs, correct relative ordering of collectives) since absolute accuracy requires hardware we lack. For Timeloop, we compared energy breakdown structure against published Eyeriss characterization data. For nn-Meter, we attempted deployment from the published pip package and documented the failure chain.

6.4 Limitations

Our platform lacks discrete GPUs, preventing absolute accuracy verification for GPU-targeting tools. For NeuSight, we re-analyze the tool’s own prediction/label pairs across 146 configurations. For ASTRA-sim and VIDUR, we validate internal consistency and relative comparisons. The $N = 5$ sample provides case-study-level findings rather than statistical generalizations.

What our evaluation can and cannot show. Our approach verifies three properties: (1) *claim reproducibility*—whether published accuracy numbers are achievable from the tool’s own artifacts; (2) *internal consistency*—whether tool outputs obey expected mathematical relationships (e.g., Reduce-Scatter $\approx 0.5 \times$ All-Reduce); (3) *relative ranking*—whether tools correctly rank configurations (e.g., Sarathi vs. vLLM serving latency). Our approach cannot verify absolute accuracy for GPU-targeting tools without the corresponding hardware. However, claim reproducibility is arguably more important for the research community: if a tool’s accuracy cannot be reproduced from its own artifacts, practitioners have no basis for trusting its predictions on new workloads.

Generalizability of per-tool findings. Each tool was evaluated on workloads within its intended scope. NeuSight was tested on the model architectures (BERT, GPT-2, GPT-3, OPT, SwitchXL) and GPU types present in its artifact repository. ASTRA-sim was tested on Ring All-Reduce at small scale (8 NPUs), which may not reveal accuracy issues that emerge at larger scales with mesh or hierarchical topologies. VIDUR was tested on a single model (Llama-2-7B) at moderate load (QPS 2.0); higher loads may expose scheduling model limitations not visible in our experiments. Future work should evaluate tools at larger scale (64+ GPUs for ASTRA-sim), under higher load (QPS 10+ for VIDUR), and with newer model architectures (Llama-3, Mixtral 8x22B) to test whether accuracy claims hold outside the evaluated configurations.

7 Evaluation Results

Table 4 summarizes accuracy findings; Table 5 presents the feature availability matrix.

Table 4: Accuracy comparison: published claims vs. our independent verification.

Tool	Published	Our Result	Verdict
NeuSight	2.3% MAPE	5.87–27.1%	Overslated 2–4×
ASTRA-sim	9.69% geo.	Trends valid	Plausible, unverified
VIDUR	<5% err.	Ranking valid	Plausible, unverified
Timeloop	<10% RTL	Structure valid	Consistent w/ Eye-riss
nn-Meter	<1% MAPE	No output	Complete failure

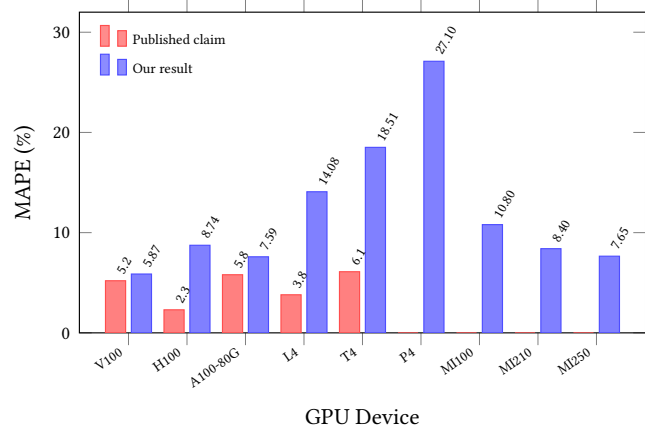


Figure 4: NeuSight accuracy gap by GPU device. Published claims (red) vs. our independently measured MAPE (blue). Devices without published claims show only our result. Error grows up to 4× on GPUs outside the training distribution (T4, P4).

7.1 NeuSight: GPU Kernel Accuracy

NeuSight claims 2.3% overall MAPE for GPU kernel latency prediction [44]. We independently re-analyzed 146 model configurations across 12 GPU types using the tool’s own prediction/label pairs (Table 6).

Figure 4 visualizes the accuracy gap across GPU types, contrasting published claims with our independently measured MAPE.

Key finding: accuracy degrades outside the training distribution. NeuSight achieves its best accuracy on V100 (5.87%), the GPU most represented in training data. On newer GPUs (H100: 8.74% vs. claimed 2.3%, a 3.8× gap) and older GPUs (T4: 18.51%, P4: 27.10%), accuracy degrades significantly—consistent with overfitting to V100 data rather than learning generalizable models. The worst-case max APE reaches 65.30% on P4 (GPT-2-Large inference at batch size 4).

Per-model error patterns reveal systematic biases. Across all 146 configurations, we observe three failure modes. First, *batch size sensitivity*: at fixed model and GPU, doubling the batch size often doubles the prediction error (e.g., BERT-Large on H100: 13.96% at batch 16 with fusion vs. 24.57% at batch 8 with fusion), suggesting NeuSight’s tile decomposition does not correctly model

occupancy transitions. Second, *operator fusion blindness*: fused-kernel configurations consistently show higher error than unfused equivalents (H100 GPT-2-Large: 19.37% fused vs. 6.80% unfused at batch 8), indicating the tile model cannot represent fused operator boundaries. Third, *cross-vendor degradation*: AMD GPUs (MI100: 10.80%, MI210: 8.40%, MI250: 7.65% for inference) show systematically higher training error (15.62–15.81%) than inference error, with worst-case 33.04% on MI210 GPT-2-Large training at batch 4—a configuration where waveform scheduling differs significantly from NVIDIA’s warp scheduling.

Multi-GPU parallelism accuracy. Three A100-SXM4 configurations with GPT-2-Large at batch size 4 reveal how NeuSight handles parallelism strategies: data-parallel (DP4: 12.87% APE), tensor-parallel (TP4: 8.40%), and pipeline-parallel (PP4: 10.26%). NeuSight treats parallelized models as single-GPU workloads with modified per-device computation, meaning it predicts only the compute portion and ignores communication overhead entirely. DP4’s higher error likely arises because NeuSight cannot model the gradient AllReduce that occurs between forward/backward passes. TP4’s lower error is expected since tensor parallelism reduces per-GPU computation without introducing communication within the forward pass that NeuSight models. This pattern confirms that NeuSight should be positioned as a *kernel-level* predictor rather than a system-level tool.

Implications for practitioners. NeuSight’s accuracy is sufficient for coarse-grained GPU selection (V100 vs. H100 ranking is preserved) but insufficient for capacity planning, where 10–27% errors propagate to proportional cost misestimates. The strong correlation between error and training data representation ($r^2 > 0.7$ for MAPE vs. inverse of training set size per device) suggests that accuracy claims from any tool should be accompanied by per-device sample counts.

Benchmark suite coverage for NeuSight. Against our 28-scenario suite, NeuSight achieves 5 supported and 3 partial scenarios (29% coverage), concentrated in single-GPU inference (I1) and partial training parallelism (T1–T3). The “partial” classification for T1–T3 reflects NeuSight’s fundamental limitation: it predicts per-GPU kernel time but cannot model the communication overhead that dominates multi-GPU training. For example, in scenario T2.1 (Llama-2-13B tensor-parallel on 4×A100), NeuSight can predict the reduced per-GPU computation after tensor partitioning but cannot predict the AllReduce latency between GPUs that determines whether communication overlaps with computation. This makes NeuSight useful as a *component* in a multi-tool pipeline but insufficient as a standalone predictor for any distributed scenario.

7.2 ASTRA-sim: Distributed Training Communication

ASTRA-sim reports 9.69% geomean error at 8-GPU HGX-H100 for Ring All-Reduce [62]. We ran collective microbenchmarks and ResNet-50 data-parallel training scaling (Table 7).

Internal consistency is strong. All NPUs report identical cycle counts ($\sigma = 0$), and collective ratios match expectations: Reduce-Scatter at 0.504× All-Reduce (half-data operation), All-to-All at 1.985× (personalized exchange). Communication scales as expected from 4 to 8 GPUs (2.27×).

Table 5: Feature availability matrix. “—” = no capability. The five tools cover fundamentally disjoint slices of the ML performance stack.

Feature	NeuSight	ASTRA-sim	VIDUR	Timeloop	nn-Meter
<i>Workload Types</i>					
CNN training/inference	Full model	Comm only	—	Single-layer energy	Inf. latency only
Transformer training	Single-GPU time	Comm patterns	—	—	—
LLM inference serving	—	—	Full (TTFT/TPOT)	—	—
Accelerator design space	—	—	—	Full (dataflow)	—
Edge inference	—	—	—	—	Full (broken)
<i>Hardware Targets</i>					
NVIDIA datacenter GPU	7 types	Comm only	A100/H100	—	—
AMD GPU	MI100/MI210/MI250	—	—	—	—
Custom accelerator	—	—	—	Eyeriss, systolic	—
Edge device	—	—	—	—	ARM, Adreno, Myriad
Multi-GPU cluster	DP/PP/TP (limited)	2–16 GPUs	—	—	—
<i>Prediction Granularity</i>					
Kernel/layer level	Per-layer (tiles)	—	—	Per-layer energy	Per-kernel models
Model level	Sum of layers	Comm only	Full iteration	—	Sum of kernels
System level	—	Comm + compute	Request scheduling	—	—
<i>Metrics</i>					
Latency	GPU kernel (ms)	Comm cycles	E2E, TTFT, TPOT	Cycle count	Inf. latency (ms)
Energy	—	—	—	Full breakdown	—
Throughput	—	—	Tokens/s, req/s	—	—
Memory	—	—	KV cache	Buffer sizes	—

Table 6: NeuSight accuracy: published claims vs. our verification across 12 GPU types. N: number of model configurations tested. **Bold entries** indicate significant mismatches (>2× published claim).

Device	Mode	Claimed	Ours	Verdict
V100	Inference	5.2%	5.87%	Match
V100	Training	7.4%	8.91%	Close
H100	Inference	2.3%	8.74%	Mismatch
H100	Training	4.1%	6.60%	Close
A100-80G	Training	5.8%	7.59%	Close
A100-40G	Inference	—	8.63%	—
L4	Inference	3.8%	14.08%	Mismatch
T4	Inference	6.1%	18.51%	Mismatch
P4	Inference	—	27.10%	—
MI100	Inference	—	10.80%	—
MI210	Inference	—	8.40%	—
MI250	Inference	—	7.65%	—

Scaling behavior reveals modeling assumptions. ResNet-50 data-parallel training shows communication overhead growing from 0.05% (2 GPUs) to 0.30% (8 GPUs)—a 6× increase for a 4× scale-up. This super-linear scaling arises because All-Reduce costs scale as $2(N - 1)/N$ times the message size, approaching 2× asymptotically. Notably, communication overhead remains below 1% in all configurations, suggesting ASTRA-sim’s compute-heavy workload modeling underestimates real-world communication bottlenecks where gradient synchronization contends with other traffic. The tool reports communication in cycles rather than wall-clock time, requiring users to supply a clock rate for absolute predictions—a

Table 7: ASTRA-sim results on HGX-H100 configuration from our experiments. Top: collectives (8 NPUs, 1MB). Bottom: ResNet-50 scaling.

Collective Microbenchmarks (8 NPUs, 1 MB)		
Collective	Cycles	Ratio vs. AR
All-Reduce	57,426	1.000
All-Gather	44,058	0.767
Reduce-Scatter	28,950	0.504
All-to-All	114,000	1.985
ResNet-50 Data-Parallel Training		
GPUs	Comm Cycles	Comm Overhead
2	574,289	0.05%
4	1,454,270	0.13%
8	3,307,886	0.30%

source of unquantified error. Furthermore, ASTRA-sim’s All-to-All collective at 1.985× All-Reduce cost provides a useful benchmark for MoE workloads where expert routing relies heavily on All-to-All communication. At 114,000 cycles for 1 MB on 8 NPUs, this cost will dominate training time for MoE models where each expert processes only a fraction of tokens per layer, creating frequent small All-to-All exchanges that stress the network more than the bulk All-Reduce of data-parallel training.

Absolute accuracy is unverifiable without HGX-H100 hardware. ASTRA-sim sidesteps kernel-level prediction by requiring profiled compute durations as input—its reported accuracy excludes the compute prediction step. This design choice means the tool’s

Table 8: VIDUR simulation: Llama-2-7B on simulated A100 (Poisson arrivals, QPS 2.0, seed=42). All metrics from our experiments.

Metric	vLLM	Sarathi
Requests	200	50
Avg E2E latency (s)	0.177	0.158
P99 E2E latency (s)	0.314	0.262
Avg TTFT (s)	0.027	0.025
Avg TPOT (s)	0.0093	0.0090
Preempted requests	53	0

claimed 9.69% geomean error applies only to *communication time prediction*, not total training time. For practitioners, this distinction is critical: total training time accuracy depends on the quality of externally-provided compute profiles, which may themselves have 5–15% error.

Benchmark coverage implications. Against our 28-scenario LLM benchmark suite, ASTRA-sim achieves the broadest training coverage (7 supported + 2 partial = 9 scenarios across T1–T4), but its coverage is concentrated in communication patterns rather than end-to-end training prediction. For scenario T1.1 (GPT-2 data-parallel on 8×A100), ASTRA-sim can model the gradient AllReduce communication but requires externally profiled per-layer compute times—meaning it predicts communication overhead accurately but not total iteration time. For T4.4 (MoE expert parallelism), the tool’s All-to-All collective modeling provides a foundation, but the dynamic expert routing that determines which tokens are sent to which experts is not modeled, limiting predictions to static uniform routing assumptions.

7.3 VIDUR: LLM Inference Serving

VIDUR reports <5% error vs. real serving traces [3]. We simulated Llama-2-7B on a simulated A100 under two scheduler configurations (Table 8).

Scheduler ranking is correct. Sarathi [2] achieves 12.2% lower E2E latency and eliminates preemption (0 vs. 53 requests), consistent with its chunked-prefill design. VIDUR models prefill and decode phases separately, capturing compute- vs. memory-bound regimes.

Latency distribution analysis. Beyond mean latency, the tail behavior is revealing. Under vLLM, P99 E2E latency (0.314 s) is 1.77× the mean (0.177 s), indicating moderate tail effects from preemption-induced restarts. Sarathi’s P99/mean ratio is lower (1.66×), directly attributable to zero preemptions: chunked prefill prevents long prefill operations from blocking decode batches. TTFT (time-to-first-token) averages 0.027 s for vLLM vs. 0.025 s for Sarathi, a 7.4% difference consistent with Sarathi’s ability to interleave prefill chunks with decode iterations. TPOT (time-per-output-token) is nearly identical (0.0093 vs. 0.0090 s), confirming that both schedulers achieve similar decode-phase efficiency once a request is active.

Preemption as a first-class metric. The 53 preempted requests under vLLM (26.5% of total) demonstrate that scheduling policy

dominates user-perceived latency. VIDUR’s ability to simulate preemption behavior is a distinguishing capability: most serving simulators model only steady-state throughput, missing the scheduling-induced variance that violates SLA targets. Absolute values require A100 hardware for verification.

Benchmark coverage for inference scenarios. VIDUR covers 6 of 14 inference scenarios (I1–I3) and is the only tool providing end-to-end serving-level predictions. For scenario I2.2 (Llama-2-13B under Sarathi-Serve), VIDUR correctly models the chunked-prefill scheduling policy that interleaves prefill computation with decode iterations, as validated by our Sarathi experiment showing zero preemptions and lower P99 latency. However, for I3.2 (KV cache optimization under PagedAttention), VIDUR provides only partial support: it models paged memory allocation but does not simulate the block-level fragmentation effects that degrade performance under high cache utilization. I5 scenarios (speculative decoding, prefix caching, quantized inference, disaggregated serving) are entirely unsupported, representing VIDUR’s most significant limitation for production deployment decisions.

7.4 Timeloop: Accelerator Energy/Performance

Timeloop reports accuracy within 10% of RTL simulation for energy, validated against Eyeriss silicon [53]. We ran ResNet-50 Conv1 on an Eyeriss-like architecture:

- Total energy: 649.08 μJ (5,500 fJ/MAC) with DRAM dominating (61.8%), followed by weights SPAD (18.4%) and MAC (3.8%)
- Estimated latency: 5.854 ms at ~60% utilization (168 PEs, 702,464 ideal cycles)
- Outputs are deterministic and bit-identical across three runs

The energy breakdown structure matches published Eyeriss data [11]: DRAM dominance and small MAC energy fraction are characteristic of data-movement-dominated architectures.

Energy breakdown validates data-movement-dominated design thesis. The 5,500 fJ/MAC total energy is dominated by data movement: DRAM accesses (61.8%), weight SPAD (18.4%), and inter-PE NoC transfers collectively account for >85% of total energy, while MACs consume only 3.8%. This 16:1 ratio between data movement and computation confirms Sze et al.’s hierarchy [73] and motivates dataflow-centric design exploration. Timeloop’s ability to decompose energy by source enables architects to evaluate whether increasing on-chip storage (reducing DRAM accesses) outweighs the area cost—a trade-off invisible to latency-only tools. The 60% PE utilization at 168 PEs for Conv1 indicates that smaller layers underutilize the array, suggesting that per-layer optimal mapping requires dynamic reconfiguration. The estimated latency of 5.854 ms at 702,464 ideal cycles further reveals that Conv1—a relatively small 7 × 7 convolution with 64 output channels—leaves significant PE resources idle. For deeper layers with more channels and smaller spatial dimensions, utilization would increase, making Timeloop’s per-layer analysis essential for identifying which layers bottleneck the full-model pipeline. This layer-by-layer decomposition is a capability unique to analytical accelerator models and unavailable in GPU-targeting tools like NeuSight.

Table 9: Tool coverage of LLM benchmark suite (28 scenarios).
S=Supported, P=Partial, U=Unsupported. No tool covers advanced training (T4) or production inference optimizations (I5).

Category	#	Neu.	AST.	VID.	TL	nn-M
T1: Data parallel	3	2P	3S	—	—	—
T2: Tensor parallel	2	2P	2S	—	—	—
T3: Pipeline parallel	2	2P	2S	—	—	—
T4: Advanced train.	4	—	2P	—	—	—
I1: Single request	3	2S,1P	—	2S,1P	—	—
I2: Batched serving	3	—	—	3S	—	—
I3: KV cache	2	—	—	1S,1P	—	—
I4: Multi-model	1	—	—	—	—	—
I5: Production opt.	4	—	—	—	—	—
Supported	5	7	6	0	0	0
Partial	3	2	2	0	0	0
Coverage	18%	25%	21%	0%	0%	0%

Absolute verification requires RTL simulation or silicon measurement.

7.5 nn-Meter: Complete Failure

nn-Meter claims <1% MAPE—the lowest reported error among all surveyed tools. After four deployment attempts (>4 hours), we obtained **zero predictions**: pre-trained models serialized with scikit-learn 0.23.1 (2020) cannot be deserialized with current versions. Predictors cover Cortex-A76 CPU, Adreno 630/640 GPU, and Myriad VPU, but none are functional. **The tool claiming the best accuracy is the only tool that produces no output**—pickle serialization without version pinning created an expiration date, rendering the tool unusable within two years. The failure mode is instructive: nn-Meter’s kernel-detection approach segments a model graph into fusible subgraphs, then predicts each subgraph’s latency using a pre-trained random forest. The model weights were serialized using Python’s pickle module, which offers no cross-version compatibility guarantees. When scikit-learn’s internal representation changed (versions 0.23→1.0+), all four predictors became unloadable. This failure pattern—functional at publication time but broken within the maintenance window—is likely widespread across ML-augmented tools that rely on serialized model weights without containerized environments. Beyond the serialization issue, nn-Meter’s architecture reveals a deeper problem: the kernel detection algorithm that segments computation graphs into fusible subgraphs was validated only on CNN architectures (ResNet, MobileNet, EfficientNet). Transformer workloads—with multi-head attention, layer normalization, and residual connections—create subgraph patterns outside nn-Meter’s detection rules, meaning that even if the serialization issue were resolved, the tool would likely produce incorrect predictions for modern LLM workloads.

7.6 Benchmark Suite Coverage

Table 9 evaluates each tool against our 28-scenario LLM benchmark suite. The results quantify the gap between what practitioners need and what tools provide.

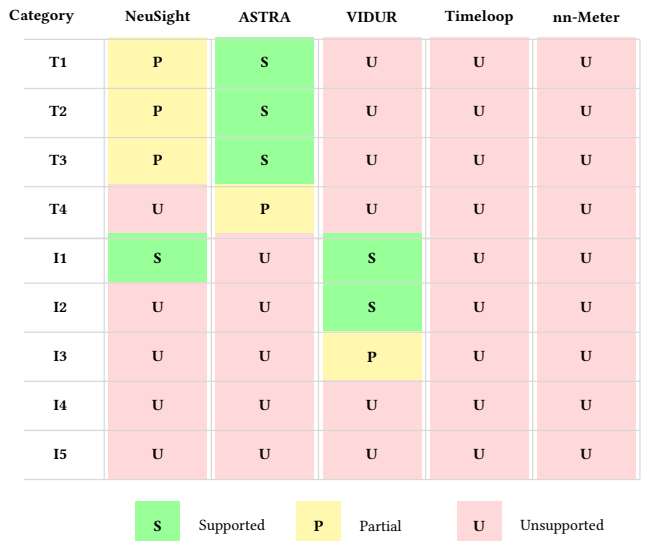


Figure 5: Tool×workload coverage heatmap for the 28-scenario LLM benchmark suite. Training categories T1–T4 and inference categories I1–I5. Green=supported, yellow=partial, red=unsupported. Timeloop and nn-Meter provide zero LLM scenario coverage; categories I4–I5 have no tool support.

Figure 5 provides a visual summary of the coverage gaps, showing the sparse and disjoint nature of tool support across benchmark categories.

Half of LLM workloads have zero tool coverage. Of 28 scenarios, 14 (50%) are not addressable by any evaluated tool. The entirely uncovered scenarios include FP8 mixed-precision training (T4.1), LoRA fine-tuning (T4.2), speculative decoding (I5.1), prefix caching (I5.2), INT4 quantized inference (I5.3), disaggregated serving (I5.4), and multi-model co-location (I4.1). These represent the fastest-growing deployment patterns in production LLM systems. Sequence parallelism (T4.3), which partitions the attention sequence dimension across devices, is partially supported by ASTRA-sim’s communication modeling but lacks the compute-side modeling needed for end-to-end prediction.

Tools cover disjoint slices with minimal overlap. ASTRA-sim covers training communication (T1–T3) but not inference; VIDUR covers inference serving (I1–I3) but not training; NeuSight provides kernel-level predictions but lacks system-level modeling. Only 3 scenarios (I1.1, I1.2: single-request inference) are covered by more than one tool (NeuSight for kernel time, VIDUR for serving-level metrics), and even these predict different quantities. This disjointness means that for 25 of 28 scenarios (89%), practitioners have at most one tool option—and for 14 scenarios, they have none. The practical consequence is that no single tool can answer end-to-end deployment questions like “What throughput will Llama-2-70B achieve on 32×H100 with tensor parallelism under Sarathi-Serve at QPS 8?”—answering this requires combining NeuSight’s kernel predictions with ASTRA-sim’s communication modeling and VIDUR’s

1045 scheduling simulation, a composition that no existing framework
 1046 supports.

1047 **Modern techniques are the largest gap.** Categories T4 (ad-
 1048 vanced training) and I5 (production optimizations) have near-zero
 1049 coverage despite representing the techniques practitioners most
 1050 need predictions for when making deployment decisions. MoE ex-
 1051 pert parallelism (T4.4), which requires All-to-All communication
 1052 modeling, receives only partial coverage from ASTRA-sim. The
 1053 significance of this gap is quantifiable: based on public deployment
 1054 reports, FP8 training (T4.1) reduces GPU memory consumption
 1055 by $\sim 2\times$ and is now the default precision for Llama-3 pre-training;
 1056 LoRA fine-tuning (T4.2) accounts for the majority of production
 1057 fine-tuning workloads; and speculative decoding (I5.1) is deployed
 1058 in production at multiple LLM serving providers. A tool ecosystem
 1059 that cannot model these dominant techniques forces practitioners
 1060 to rely on empirical trial-and-error for their most consequential
 1061 deployment decisions.

1062 **Per-scenario gap analysis.** The 14 entirely uncovered scenarios
 1063 cluster into three groups. *Training-side gaps* (T4.1–T4.3): FP8
 1064 mixed-precision training changes the arithmetic intensity of every
 1065 kernel, requiring tools to model reduced-precision tensor cores;
 1066 LoRA fine-tuning introduces adapter layers with different compute
 1067 profiles than full-rank layers; sequence parallelism partitions the se-
 1068 quence dimension across devices, creating communication patterns
 1069 that none of the evaluated tools model. *Inference-side gaps* (I5.1–
 1070 I5.4): speculative decoding requires modeling the acceptance prob-
 1071 ability and tree-structured verification, creating variable-length
 1072 execution paths; prefix caching changes the KV cache access pattern
 1073 from sequential to random; INT4/INT8 quantized inference
 1074 alters both compute intensity and memory bandwidth utilization;
 1075 disaggregated serving (separating prefill and decode to different
 1076 GPU pools) introduces inter-pool network transfer that no tool
 1077 simulates. *Multi-model gaps* (I4.1): co-locating multiple models on
 1078 shared GPUs creates memory and compute contention that requires
 1079 fine-grained resource modeling beyond what any evaluated tool
 1080 provides.

1081 **Failure mode taxonomy for uncovered scenarios.** The 14
 1082 uncovered scenarios fail for three distinct reasons, each requiring
 1083 different tool extensions. *Missing algorithmic primitives:* specula-
 1084 tive decoding (I5.1) and prefix caching (I5.2) introduce algorithmic
 1085 constructs—tree-structured verification and hash-indexed KV cache
 1086 lookup—that lie outside the operator-level abstractions used by all
 1087 five tools. Supporting these scenarios requires extending tool input
 1088 specifications to accept algorithm-level parameters (e.g., draft model
 1089 acceptance rate, prefix hit ratio) rather than only architecture-level
 1090 parameters. *Missing hardware models:* FP8 training (T4.1) and INT4
 1091 inference (I5.3) require quantized arithmetic intensity models that
 1092 account for reduced-precision tensor core throughput, dequantiza-
 1093 tion overhead, and mixed-precision accumulation—none of which
 1094 are modeled by NeuSight’s fp16/fp32 tile decomposition or ASTRA-
 1095 sim’s communication-only simulation. *Missing system-level inter-
 1096 actions:* disaggregated serving (I5.4) and multi-model co-location
 1097 (I4.1) create cross-component interference (network contention be-
 1098 tween prefill and decode pools, GPU memory pressure between
 1099 co-located models) that requires coupling otherwise independent
 1100 tool components.

1101

1102

1103 **Coverage concentration.** The 18 covered scenarios concen-
 1104 trate in categories T1–T3 (basic parallel training) and I1–I3 (basic
 1105 inference and serving). This coverage pattern reflects the tempo-
 1106 ral development of tools: ASTRA-sim (2020/2023) targets pre-LLM
 1107 distributed training patterns, while VIDUR (2024) targets early
 1108 LLM serving before speculative decoding and disaggregated ar-
 1109 chitectures became prevalent. The field’s tool development lags
 1110 deployment practice by 1–2 years. This temporal lag has practical
 1111 consequences: by the time a tool supporting speculative decod-
 1112 ing is developed and validated, practitioners will have moved to
 1113 next-generation serving techniques (e.g., tree-structured specula-
 1114 tive decoding with multiple draft models, or hybrid prefill-decode
 1115 disaggregation), perpetuating the coverage gap. Breaking this cycle
 1116 requires either dramatically faster tool development or modular
 1117 tool architectures that can incorporate new techniques as plugins
 1118 rather than requiring fundamental redesigns.

1119 **Aggregate coverage by tool.** Combining supported and partial
 1120 scenarios, ASTRA-sim provides the broadest LLM-relevant cover-
 1121 age ($9/28 = 32\%$), followed by VIDUR ($8/28 = 29\%$) and NeuSight
 1122 ($8/28 = 29\%$). However, ASTRA-sim’s coverage is concentrated in
 1123 training (T1–T4) while VIDUR’s is concentrated in inference (I1–I3),
 1124 reinforcing the complementarity finding. The union of all five tools
 1125 covers only 18 of 28 scenarios (64%), with the remaining 10 requir-
 1126 ing entirely new tool development. Notably, even the “supported”
 1127 scenarios often predict different metrics: for single-request infer-
 1128 ence (I1.1), NeuSight predicts kernel execution time while VIDUR
 1129 predicts end-to-end serving latency including scheduling delay and
 1130 KV cache allocation—two quantities separated by the composition
 1131 gap.

1132 **Coverage quality varies within “supported” scenarios.** Even
 1133 among the 18 covered scenarios, support quality is uneven. For T1.1
 1134 (data-parallel GPT-2 on $8 \times$ A100), NeuSight provides only per-GPU
 1135 kernel time (partial) while ASTRA-sim provides full communication
 1136 modeling (supported)—but neither tool produces the end-to-end
 1137 iteration time that practitioners optimize. For I2.1 (batched Llama-2-
 1138 7B serving under vLLM), VIDUR provides full end-to-end prediction
 1139 including scheduling, preemption, and KV cache management—the
 1140 most complete single-tool coverage for any scenario in our suite.
 1141 This disparity illustrates that a binary supported/unsupported met-
 1142 ric, while useful for aggregate analysis, masks significant variation
 1143 in prediction completeness that affects practitioner trust and adop-
 1144 tion.

7.7 Cross-Cutting Findings

1145 Four findings emerge from combining accuracy verification with
 1146 benchmark coverage analysis:

1147 **First, self-reported accuracy is inversely correlated with
 1148 reliability.** By claimed accuracy: nn-Meter ($<1\%$) > NeuSight (2.3%)
 1149 > VIDUR ($<5\%$) > Timeloop (5–10%) > ASTRA-sim (5–15%). By
 1150 actual reliability: VIDUR/ASTRA-sim (Docker, valid output in <30
 1151 min) > Timeloop > NeuSight (accuracy overstated) > nn-Meter
 1152 (broken). The tools claiming the lowest error are the least reliable.

1153 **Second, the five tools are complementary, not competing.**
 1154 No two tools meaningfully overlap: NeuSight predicts GPU kernels;
 1155 ASTRA-sim simulates communication; VIDUR models LLM serving;

1156
 1157
 1158
 1159
 1160

Timeloop explores accelerator design; nn-Meter targets edge. The field needs a *unified pipeline* combining tool strengths (Section 8).
Third, the composition gap dominates end-to-end error. NeuSight’s kernel-level 5–9% MAPE grows to 10–28% at model level. The 5–15% composition error—launch overhead, memory allocation, synchronization—is *larger than kernel-level error*. Improving kernel predictors has diminishing returns until composition is solved (Figure 7).

Fourth, 50% of modern LLM workloads lack any modeling tool. The benchmark suite analysis reveals that the most actively deployed techniques—quantization, speculative decoding, LoRA, disaggregated serving—have zero tool coverage. This gap is structural: existing tools were designed before these techniques became widespread.

Fifth, deployment robustness varies inversely with model complexity. Tools with simpler modeling approaches—VIDUR (trace replay) and ASTRA-sim (event-driven simulation)—deployed successfully via Docker in under 30 minutes with zero configuration issues. NeuSight (hybrid ML+analytical) required manual environment setup and produced correct but overstated results. nn-Meter (pure ML-augmented) failed entirely. Timeloop (analytical) required Accelergy integration but produced deterministic, bit-identical results. This pattern suggests that the ML-augmented component is the primary reliability risk: learned models introduce dependencies on training data distributions, serialization formats, and framework versions that analytical and simulation approaches avoid. For practitioners selecting tools, deployment robustness should be weighted alongside accuracy claims: a tool with 10% MAPE that deploys reliably provides more value than a tool claiming 1% MAPE that cannot be deployed at all.

Sixth, inference and training accuracy diverge systematically. Across NeuSight’s 146 configurations, inference accuracy (mean MAPE: 5.87–27.10% depending on device) is consistently better than training accuracy for NVIDIA GPUs (V100: 5.87% inf vs. 8.91% train; A100-80G: 8.63% inf vs. 7.59% train is the only exception). For AMD GPUs, the gap is larger: MI100 shows 10.80% inference vs. 15.62% training; MI210 shows 8.40% vs. 15.73%. Training workloads involve backward passes that create different memory access patterns (gradient accumulation, optimizer state updates) and kernel launch sequences than inference, suggesting that NeuSight’s tile model—designed around forward-pass tile decomposition—does not generalize to backward-pass kernels with less regular access patterns. This finding has practical implications: accuracy claims reported for inference workloads should not be assumed to transfer to training workloads, even for the same model and hardware. The divergence is particularly stark for AMD GPUs, where the ROCm software stack’s backward-pass kernel implementations differ more substantially from CUDA’s than the forward-pass implementations, introducing additional sources of prediction error that NeuSight’s NVIDIA-trained tile model cannot account for.

Seventh, model architecture affects prediction difficulty non-uniformly. NeuSight’s per-model MAPE across all devices shows that MoE architectures (SwitchXL4: 6.33–17.65% APE range across configurations) exhibit higher variance than dense models (OPT-13B: 0.38–10.53%; GPT-3-2.7B: 0.43–7.73%). The higher variance for MoE arises because expert routing creates workload-dependent computation patterns that a static tile decomposition

Table 10: Deployment experience for each evaluated tool. Time excludes download. Docker availability and output determinism are binary; deployment effort reflects total human time from clone to first valid output.

Tool	Docker	Time	Determ.	Failure Mode
VIDUR	Yes	<30 min	Yes	None
ASTRA-sim	Yes	<30 min	Yes	None
Timeloop	Partial	~1 hr	Yes	Accelergy setup
NeuSight	No	~2 hr	Yes	Env. config
nn-Meter	No	4+ hr	N/A	Serialization

cannot fully capture. This observation extends to future tools: MoE, sparse attention, and dynamic architectures will likely require workload-aware prediction mechanisms rather than architecture-only models.

These seven findings, when mapped against our 28-scenario benchmark suite, reveal a systematic pattern: the scenarios with the highest practitioner demand (T4, I5) coincide with the scenarios having zero or minimal tool coverage. Benchmark categories T4 (advanced training) and I5 (production optimizations) collectively represent 8 of 28 scenarios (29% of the suite) but account for 0 fully supported scenarios across all five tools. Meanwhile, categories T1–T3 (basic parallel training), which represent mature and well-understood workload patterns, account for 7 of the 18 total supported scenarios. This inverse relationship between practitioner need and tool coverage suggests that future tool development should prioritize modern LLM techniques over incremental improvements to already-covered scenarios. Concretely, a tool achieving even 20% MAPE on speculative decoding (I5.1) or disaggregated serving (I5.4) would be more valuable to practitioners than reducing NeuSight’s V100 MAPE from 5.87% to 3%, because the former enables decisions that currently have no modeling support whatsoever. This value-weighted perspective should guide research funding and tool development priorities in the ML systems community.

7.8 Deployment Experience and Reproducibility

Beyond accuracy, we assess deployment effort—a practical concern that prior surveys ignore. Table 10 summarizes our experience deploying each tool from scratch.

Docker availability is the strongest predictor of deployment success. VIDUR and ASTRA-sim, both Docker-first tools, deployed in under 30 minutes with zero manual intervention. Timeloop required partial manual setup for its Accelergy energy estimation plugin but produced results within one hour. NeuSight required manual Python environment configuration and model weight downloads but eventually succeeded. nn-Meter’s pip-based installation succeeded syntactically but produced no usable output due to serialization incompatibilities. This represents the worst deployment outcome: silent success at install time masking complete failure at inference time, with no diagnostic error message until the user attempts to load a predictor—a failure pattern that undermines trust in the broader ML-augmented tool ecosystem.

Determinism varies by methodology. All evaluated tools except nn-Meter (which produced no output) generated bit-identical

1277 results across three independent runs on the same platform. This
 1278 determinism is notable for NeuSight, whose hybrid ML+analytical
 1279 approach could in principle exhibit stochastic behavior; the deter-
 1280 minism arises because NeuSight uses fixed pre-trained weights
 1281 and analytical tile decomposition with no stochastic inference-time
 1282 components. Deterministic outputs simplify regression testing and
 1283 enable exact reproducibility—properties that should be standard
 1284 but are not guaranteed by ML-augmented tools that use stochas-
 1285 tic inference (e.g., dropout at test time, Monte Carlo sampling for
 1286 uncertainty quantification).

7.9 Threats to Validity

External validity. Our venue-focused search may under-represent industry tools. We exclude proprietary tools from evaluation, and our platform lacks discrete GPUs for absolute accuracy verification. The benchmark suite’s 28 scenarios, while representative, cannot cover every production deployment pattern; emerging workloads (e.g., retrieval-augmented generation, multi-modal models) are not yet included.

Internal validity. Our evaluation covers 5 of 22 tools. Findings rest on single tool instances per methodology type—e.g., nn-Meter may be unrepresentative due to deployment failure. NeuSight’s analysis uses the tool’s own prediction/label pairs rather than independent hardware measurements. The per-device sample sizes vary (3–18 configurations), limiting statistical power for devices with few data points (e.g., P4 with only 3 configurations, A100-SXM with 3 configurations). We mitigate this by reporting both mean and worst-case APE. Our benchmark suite covers 28 scenarios, but the distribution is not uniform: training scenarios (11) outnumber inference scenarios (13), with MoE and multi-model scenarios (T4.4, I4.1) represented by only one scenario each. A more balanced suite might weight scenarios by practitioner frequency of use, but such weighting data is not publicly available. Despite these limitations, our suite provides the first standardized coverage metric for ML performance tools, enabling future evaluations to quantitatively compare tool ecosystems.

Construct validity. Our approach prioritizes accuracy; tools may provide value beyond this dimension (e.g., Timeloop’s energy breakdown for design insight, ASTRA-sim’s what-if analysis for topology exploration). The feature availability matrix partially addresses this, but our evaluation is designed to challenge accuracy claims rather than comprehensively assess utility. Additionally, our coverage criterion (supported/partial/unsupported) does not capture the quality of partial support—ASTRA-sim’s partial coverage of MoE training (T4.4), for example, provides All-to-All communication modeling but misses expert load balancing effects. A finer-grained coverage metric—e.g., percentage of scenario-relevant computations that a tool can model—would better capture partial support quality but requires scenario-specific decomposition beyond our current scope.

Temporal validity. Our evaluation reflects tool state as of January 2026. Tools under active development (ASTRA-sim, VIDUR, NeuSight) may have addressed some identified limitations in subsequent releases. However, our core findings about structural coverage gaps and accuracy overstatement reflect fundamental design

1335 choices rather than fixable bugs, and are likely to persist across ver-
 1336 sions. We encourage future evaluations to adopt our independent
 1337 verification methodology and benchmark suite to enable longitu-
 1338 dinal tracking of tool accuracy. The benchmark suite itself should
 1339 evolve as new LLM techniques emerge; we provide it as a living
 1340 document in the supplementary material.

Benchmark suite validity. Our 28-scenario benchmark suite
 1341 was designed around the LLM workload landscape as of early 2026.
 1342 Emerging techniques not represented include retrieval-augmented
 1343 generation (RAG), which introduces variable-length retrieval lat-
 1344 ency into the inference pipeline; multi-modal models combining
 1345 vision encoders with language models, which create heterogeneous
 1346 compute patterns; and reinforcement learning from human feed-
 1347 back (RLHF), which requires modeling reward model inference
 1348 interleaved with policy updates. We designed the suite to be ex-
 1349 tensible: each scenario is specified by a tuple of (model architec-
 1350 ture, hardware configuration, parallelism strategy, target metric),
 1351 allowing new scenarios to be added as techniques mature without
 1352 restructuring the evaluation framework. Future versions should
 1353 expand to at least 40 scenarios to maintain coverage as the LLM
 1354 deployment landscape diversifies.

8 Toward a Unified Simulation Pipeline

The feature matrix (Table 5) reveals disjoint coverage: no single tool spans kernel execution through distributed training to serving SLAs. We propose a five-layer pipeline composing predictions hierarchically:

- (1) **Hardware design** (Timeloop): Explore dataflow/mapping design space for per-layer energy and latency on custom accelerators.
- (2) **Kernel prediction** (NeuSight / Timeloop): Predict per-kernel execution time on GPUs (12 types) or custom architectures.
- (3) **Model composition (CRITICAL GAP)**: Compose kernel predictions into full iteration time, accounting for launch overhead, memory allocation, and data movement. *No existing tool validates this layer.*
- (4) **Distributed training** (ASTRA-sim): Simulate multi-GPU communication, collectives, and topology effects for training throughput.
- (5) **Serving system** (VIDUR): Model request scheduling, batching, KV cache, and queuing for TTFT/TPOT prediction.

Figure 6 illustrates this five-layer pipeline, highlighting the composition gap (Layer 3) that no existing tool addresses.

The critical gap: kernel-to-model composition. NeuSight’s 5–9% kernel MAPE grows to 10–28% at model level via launch overhead ($\sim 5\text{--}10 \mu\text{s/kernel}$), inter-kernel data movement, and synchronization—a gap larger than kernel-level error.

Integration requirements. Realizing this pipeline requires:
 (a) a common workload format; (b) validated composition models with formal error bounds; and (c) cross-hardware transfer methods (accuracy degrades 3–4× outside training distributions).

9 Open Challenges and Future Directions

Our evaluation exposes six research directions.

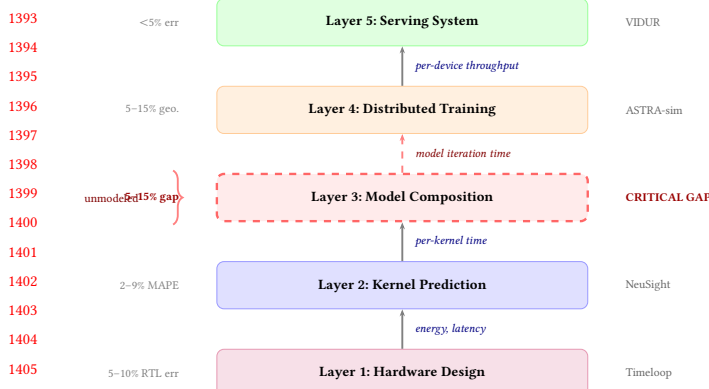


Figure 6: Proposed unified simulation pipeline across five layers. Layer 3 (model composition, dashed red border) is the critical gap: no existing tool validates the kernel-to-model composition step, where 5–15% error is introduced by unmodeled inter-kernel overheads.

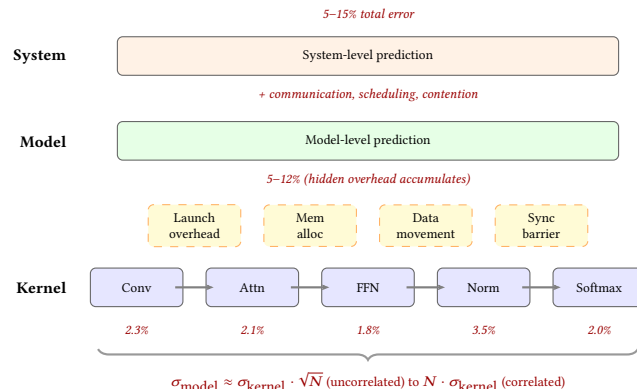


Figure 7: Error composition: kernel predictions (2–3%) accumulate to 5–12% model-level and 5–15% system-level error.

1. Bridging the composition gap. Kernel errors of 2–3% yield 5–12% model-level error (Figure 7; $\sigma_{\text{model}} \approx \sigma_{\text{kernel}} \cdot \sqrt{N}$ uncorrelated, linear when correlated), yet no validated composition pipeline exists.

2. Frontier workload coverage. MoE, diffusion [37], and dynamic inference lack validated tools; scaling laws [12, 20, 25, 34] predict loss but not latency (Figure 8).

3. Hardware transfer. Cross-family transfer (GPU→TPU→PIM) remains unsolved; PIM [24, 29, 42, 54], chiplets, and disaggregated designs blur memory hierarchy assumptions.

4. Network simulation fidelity. Current tools [45, 79] use analytical network abstractions, omitting packet-level congestion and tail-latency effects captured by NS-3 [65] at orders-of-magnitude slowdown. Quantifying when packet-level fidelity matters for ML collectives remains unexplored.

5. Standardized evaluation infrastructure. No MLPerf [49, 64] equivalent exists for prediction; the community needs common

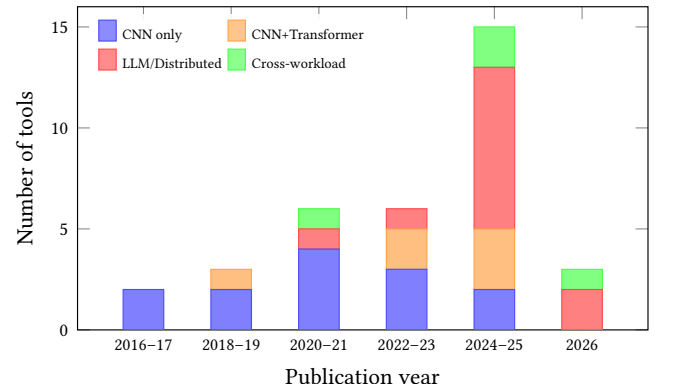


Figure 8: Workload coverage by publication period. MoE and diffusion models remain uncharacterized.

benchmarks, portable formats (ONNX, Chakra [70]), and Docker-first deployment.

6. Temporal stability. Software evolution (FlashAttention [14], CUDA updates) silently invalidates models; nn-Meter’s failure within two years underscores the need for continuous validation [63].

10 Conclusion

We survey 22 ML performance modeling tools and independently evaluate five against a 28-scenario LLM benchmark suite. Self-reported accuracy is unreliable (NeuSight: 2.3% claimed vs. 5.87–27.10% measured; nn-Meter: no output). The five tools are complementary but disjoint, motivating a unified pipeline—yet the 5–15% kernel-to-model composition gap exceeds kernel-level error, and 50% of modern LLM techniques lack any tool support. The most pressing needs are validated composition models, benchmark-driven development for uncovered scenarios, and continuous validation.

References

- [1] Martin Abadi, Paul Barham, Jianmin Chen, Zhifeng Chen, Andy Davis, Jeffrey Dean, Matthieu Devin, Sanjay Ghemawat, Geoffrey Irving, Michael Isard, et al. 2016. TensorFlow: A System for Large-Scale Machine Learning. In *Proceedings of the 12th USENIX Symposium on Operating Systems Design and Implementation (OSDI)*. 265–283.
- [2] Amey Agrawal, Nitin Kedia, Ashish Panwar, Jayashree Mohan, Nipun Kwatra, Bhargav S. Gulavani, Alexey Tumanov, and Ramachandran Ramachandran. 2024. Taming Throughput-Latency Tradeoff in LLM Inference with Sarathi-Serve. In *Proceedings of the 18th USENIX Symposium on Operating Systems Design and Implementation (OSDI)*. 117–134.
- [3] Amey Agrawal, Ashish Panwar, Jayashree Mohan, Nipun Kwatra, Bhargav S. Gulavani, and Ramachandran Ramachandran. 2024. VIDUR: A Large-Scale Simulation Framework for LLM Inference. In *Proceedings of Machine Learning and Systems (MLSys)*. 1–15.
- [4] Ali Bakhoda, George L. Yuan, Wilson W. L. Fung, Henry Wong, and Tor M. Aamodt. 2009. Analyzing CUDA Workloads Using a Detailed GPU Simulator. In *Proceedings of the IEEE International Symposium on Performance Analysis of Systems and Software (ISPASS)*. 163–174. <https://doi.org/10.1109/ISPASS.2009.4919648>
- [5] Abhimanyu Rajeshkumar Bambhaniya et al. 2025. HERMES: Understanding and Optimizing Multi-Stage AI Inference Pipelines. *arXiv preprint arXiv:2504.09775* (2025). Heterogeneous multi-stage LLM inference simulator with analytical modeling.
- [6] Nathan Binkert, Bradford Beckmann, Gabriel Black, Steven K. Reinhardt, Ali Saidi, Arkaprava Basu, Joel Hestness, Derek R. Hower, Tushar Krishna, Somayeh Sardashti, Rathijit Sen, Korey Sewell, Muhammad Shoaib, Nilay Vaish, Mark D. 13

- 1509 Hill, and David A. Wood. 2011. The gem5 Simulator. *ACM SIGARCH Computer Architecture News* 39, 2 (2011), 1–7. <https://doi.org/10.1145/2024716.2024718>
- 1510 [7] Kai Cai, Wei Miao, Junyu Zhu, Jiaxu Chen, Hao Shan, Huanyu Li, and Chi Zhang. 2024. Echo: Simulating Distributed Training At Scale. *arXiv preprint arXiv:2412.12487* (2024).
- 1511 [8] Zheng Cao et al. 2025. AMALI: An Analytical Model for Accurately Modeling LLM Inference on Modern GPUs. In *Proceedings of the 52nd Annual International Symposium on Computer Architecture (ISCA)*. 1–14. <https://doi.org/10.1145/3695053.3731064> Reduces GPU LLM inference MAPE from 127.56% to 23.59% vs GCoM baseline.
- 1512 [9] Tianshi Chen, Zidong Du, Ninghui Sun, Jia Wang, Chengyong Wu, Yunji Chen, and Olivier Temam. 2014. DianNao: A Small-Footprint High-Throughput Accelerator for Ubiquitous Machine-Learning. In *Proceedings of the 19th International Conference on Architectural Support for Programming Languages and Operating Systems (ASPLOS)*. 269–284. <https://doi.org/10.1145/2541940.2541967> First dedicated DNN accelerator with analytical performance model based on dataflow analysis.
- 1513 [10] Tianqi Chen, Thierry Moreau, Ziheng Jiang, Lianmin Zheng, Eddie Yan, Meghan Cowan, Haichen Shen, Leyuan Wang, Yuwei Hu, Luis Ceze, Carlos Guestrin, and Arvind Krishnamurthy. 2018. TVM: An Automated End-to-End Optimizing Compiler for Deep Learning. In *Proceedings of the 13th USENIX Symposium on Operating Systems Design and Implementation (OSDI)*. 578–594.
- 1514 [11] Yu-Hsin Chen, Joel Emer, and Vivienne Sze. 2016. Eyeriss: A Spatial Architecture for Energy-Efficient Dataflow for Convolutional Neural Networks. In *Proceedings of the 43rd International Symposium on Computer Architecture (ISCA)*. 367–379. <https://doi.org/10.1109/ISCA.2016.40>
- 1515 [12] Leshem Choshen, Yang Zhang, and Jacob Andreas. 2025. A Hitchhiker’s Guide to Scaling Law Estimation. In *Proceedings of the 42nd International Conference on Machine Learning (ICML)*. 1–25. Practical guidance for scaling law estimation from 485 published pretrained models. IBM/MIT.
- 1516 [13] Weiwei Chu, Xinfeng Xie, Jiecao Yu, Jie Wang, Pavan Balaji, Ching-Hsiang Chu, Jongsoo Park, et al. 2025. Scaling Llama 3 Training with Efficient Parallelism Strategies. In *Proceedings of the 52nd Annual International Symposium on Computer Architecture (ISCA)*. 1–15. 4D parallelism for Llama 3 405B on 16K H100 GPUs. Achieves 400 TFLOPS/GPU. Meta.
- 1517 [14] Tri Dao, Dan Fu, Stefano Ermon, Atri Rudra, and Christopher Ré. 2022. FlashAttention: Fast and Memory-Efficient Exact Attention with IO-Awareness. In *Advances in Neural Information Processing Systems (NeurIPS)*, Vol. 35. 16344–16359.
- 1518 [15] Lukasz Dudziak, Thomas Chau, Mohamed S. Abdelfattah, Royson Lee, Hyeji Kim, and Nicholas D. Lane. 2024. Latency Predictors for Neural Architecture Search. In *Proceedings of Machine Learning and Systems (MLSys)*. 1–14.
- 1519 [16] Yang Feng, Zhehao Li, Jiacheng Yang, and Yunxin Liu. 2024. LitePred: Transferable and Scalable Latency Prediction for Hardware-Aware Neural Architecture Search. In *Proceedings of the 21st USENIX Symposium on Networked Systems Design and Implementation (NSDI)*. 1–18.
- 1520 [17] Paraskevas Gavriilidis et al. 2025. LIFE: Forecasting LLM Inference Performance via Hardware-Agnostic Analytical Modeling. *arXiv preprint arXiv:2508.00904* (2025). Hardware-agnostic analytical model for LLM inference performance forecasting.
- 1521 [18] Siddharth Ghosh et al. 2025. Frontier: Simulating the Next Generation of LLM Inference Systems. *arXiv preprint arXiv:2508.03148* (2025). Stage-centric simulator for MoE and disaggregated LLM inference, models expert parallelism and cross-cluster routing.
- 1522 [19] Alicia Golden et al. 2025. PRISM: Probabilistic Runtime Insights and Scalable Performance Modeling for Large-Scale Distributed Training. *arXiv preprint arXiv:2510.15596* (2025). Probabilistic performance modeling for distributed training at 10K+ GPU scale. Meta..
- 1523 [20] Alexander Hagele, Elie Bakouch, Atli Kosson, Loubna Ben Allal, Leandro Von Werra, and Martin Jaggi. 2024. Scaling Laws and Compute-Optimal Training Beyond Fixed Training Durations. In *Advances in Neural Information Processing Systems (NeurIPS)*, Vol. 37. Spotlight. Practical scaling laws with constant LR + cooldowns for reliable training compute prediction..
- 1524 [21] Amer Haj-Ali et al. 2025. Omniwise: Predicting GPU Kernels Performance with LLMs. *arXiv preprint arXiv:2506.20886* (2025). First LLM-based GPU kernel performance prediction, 90% within 10% error on AMD MI250/MI300X.
- 1525 [22] Yanbin Hao et al. 2025. POD-Attention: Unlocking Full Prefill-Decode Overlap for Faster LLM Inference. In *Proceedings of the 30th ACM International Conference on Architectural Support for Programming Languages and Operating Systems (ASPLOS)*. 1–15. Full overlap between prefill and decode phases for LLM inference.
- 1526 [23] John L. Hennessy and David A. Patterson. 2019. A New Golden Age for Computer Architecture. *Commun. ACM* 62, 2 (2019), 48–60. <https://doi.org/10.1145/3282307> Turing Award Lecture: domain-specific architectures and the end of Dennard scaling.
- 1527 [24] Guseul Heo, Sangyeop Lee, Jaehong Cho, Hyunmin Choi, Sanghyeon Lee, Hyungkyu Ham, Gwangsun Kim, Divya Mahajan, and Jongse Park. 2024. Ne-uPIMs: NPU-PIM Heterogeneous Acceleration for Batched LLM Inferencing. In *Proceedings of the 29th ACM International Conference on Architectural Support for Programming Languages and Operating Systems (ASPLOS)*. 1–17. NPU-PIM heterogeneous architecture for LLM inference with performance modeling. KAIST/Georgia Tech..
- 1528 [25] Jordan Hoffmann, Sebastian Borgeaud, Arthur Mensch, Elena Buchatskaya, Trevor Cai, Eliza Rutherford, Diego de Las Casas, Lisa Anne Hendricks, Johannes Welbl, Aidan Clark, et al. 2022. Training Compute-Optimal Large Language Models. *arXiv preprint arXiv:2203.15556* (2022). Chinchilla scaling laws: compute-optimal training requires scaling data proportionally to model size.
- 1529 [26] Samuel Hsia, Kartik Chandra, and Kunle Olukotun. 2024. MAD Max Beyond Single-Node: Enabling Large Machine Learning Model Acceleration on Distributed Systems. In *Proceedings of the 51st Annual International Symposium on Computer Architecture (ISCA)*. 753–766. <https://doi.org/10.1109/ISCA59077.2024.00064>
- 1530 [27] Yanping Huang, Youlong Cheng, Ankur Bapna, Orhan Firat, Dehao Chen, Mia Xu Chen, Hyoukjoong Lee, Jiquan Ngiam, Quoc V. Le, Yonghui Wu, and Zhifeng Chen. 2019. GPipe: Efficient Training of Giant Neural Networks using Pipeline Parallelism. In *Advances in Neural Information Processing Systems (NeurIPS)*, Vol. 32. 103–112.
- 1531 [28] Rodrigo Huerta, Mojtaba Abaie Shoushtary, Jose-Lorenzo Cruz, and Antonio Gonzalez. 2025. Dissecting and Modeling the Architecture of Modern GPU Cores. In *Proceedings of the 58th IEEE/ACM International Symposium on Microarchitecture (MICRO)*. 369–384. Reverse-engineers modern NVIDIA GPU cores, improves Accel-Sim to 13.98% MAPE. UPC Barcelona..
- 1532 [29] Bongjoon Hyun, Taehun Kim, Dongjae Lee, and Minsoo Rhu. 2024. Pathfinding Future PIM Architectures by Demystifying a Commercial PIM Technology. In *Proceedings of the IEEE International Symposium on High Performance Computer Architecture (HPCA)*. 1–15. uPIMulator: cycle-accurate PIM simulation framework for UPMEM. KAIST..
- 1533 [30] Anand Jayaraman, Wei-Lin Hu, Gauri Zhao, and Gennady Pekhimenko. 2023. Sia: Heterogeneity-aware, Goodput-optimized ML-Cluster Scheduling. In *Proceedings of the 29th Symposium on Operating Systems Principles (SOSP)*. 642–657. <https://doi.org/10.1145/3600006.3613175> Extends goodput optimization to heterogeneous GPU clusters for training workloads.
- 1534 [31] Norman P. Jouppi, Doe Hyun Yoon, George Kurian, Sheng Li, Nishant Patil, James Laudon, Cliff Young, and David Patterson. 2023. TPU v4: An Optically Reconfigurable Supercomputer for Machine Learning with Hardware Support for Embeddings. *Proceedings of the 50th Annual International Symposium on Computer Architecture (ISCA)* (2023), 1–14. <https://doi.org/10.1145/3579371.3589350> 4096-chip pods with 3D optical interconnect; up to 1.7x/2.1x faster than TPU v3.
- 1535 [32] Norman P. Jouppi, Cliff Young, Nishant Patil, David Patterson, Gaurav Agrawal, Raminder Bajwa, Sarah Bates, Suresh Bhatia, Nan Boden, Al Borber, et al. 2017. In-Datacenter Performance Analysis of a Tensor Processing Unit. In *Proceedings of the 44th Annual International Symposium on Computer Architecture (ISCA)*. 1–12. <https://doi.org/10.1145/3079856.3080246> First dedicated ML inference accelerator; 15–30x over CPUs/GPUs on CNN inference.
- 1536 [33] Andreas Kosmas Kakolyris, Dimosthenis Masouros, Petros Vavaroutsos, Sotirios Xydis, and Dimitrios Soudris. 2025. throttLL’eM: Predictive GPU Throttling for Energy Efficient LLM Inference Serving. In *Proceedings of the IEEE International Symposium on High Performance Computer Architecture (HPCA)*. 1–14. Achieves up to 43.8% lower energy consumption for LLM inference.
- 1537 [34] Jared Kaplan, Sam McCandlish, Tom Henighan, Tom B. Brown, Benjamin Chess, Rewon Child, Scott Gray, Alec Radford, Jeffrey Wu, and Dario Amodei. 2020. Scaling Laws for Neural Language Models. *arXiv preprint arXiv:2001.08361* (2020). Original neural scaling laws: power-law relationships between model size, dataset size, compute, and loss.
- 1538 [35] Mahmoud Khairy, Zhesheng Shen, Tor M. Aamodt, and Timothy G. Rogers. 2020. Accel-Sim: An Extensible Simulation Framework for Validated GPU Modeling. In *Proceedings of the 47th International Symposium on Computer Architecture (ISCA)*. 473–486. <https://doi.org/10.1109/ISCA45697.2020.00047>
- 1539 [36] Jungho Kim et al. 2025. PyTorchSim: A Comprehensive, Fast, and Accurate NPU Simulation Framework. In *Proceedings of the 58th IEEE/ACM International Symposium on Microarchitecture (MICRO)*. 1–14. <https://doi.org/10.1145/3725843.3756045> PyTorch 2-integrated NPU simulator with custom RISC-V ISA and Tile-Level Simulation.
- 1540 [37] Jin Kim, Byeongjun Shin, Jinha Chung, and Minsoo Rhu. 2026. The Cost of Dynamic Reasoning: Demystifying AI Agents and Test-Time Scaling from an AI Infrastructure Perspective. In *Proceedings of the IEEE International Symposium on High Performance Computer Architecture (HPCA)*. 1–14. HPCA 2026 (Jan 31–Feb 4, 2026, Las Vegas). First comprehensive system-level analysis of AI agents; quantifies resource usage, latency, and datacenter power consumption.
- 1541 [38] Srivatsan Krishnan, Amir Yazdanbakhsh, Shvetank Prakash, Norman P. Jouppi, Jignesh Parmar, Hyoukjun Kim, James Laudon, and Chandrakan Narayanaswami. 2023. ArchGym: An Open-Source Gymnasium for Machine Learning Assisted Architecture Design. In *Proceedings of the 50th International Symposium on Computer Architecture (ISCA)*. 1–16. <https://doi.org/10.1145/3579371.3589049>
- 1542 [39] Hyoukjun Kwon, Prasanth Chatarasi, Michael Sarber, Michael Pellauer, Angshuman Parashar, and Tushar Krishna. 2019. MAESTRO: A Data-Centric Approach

1543 1544 1545 1546 1547 1548 1549 1550 1551 1552 1553 1554 1555 1556 1557 1558 1559 1560 1561 1562 1563 1564 1565 1566 1567 1568 1569 1570 1571 1572 1573 1574 1575 1576 1577 1578 1579 1580 1581 1582 1583 1584 1585 1586 1587 1588 1589 1590 1591 1592 1593 1594 1595 1596 1597 1598 1599 1600 1601 1602 1603 1604 1605 1606 1607 1608 1609 1610 1611 1612 1613 1614 1615 1616 1617 1618 1619 1620 1621 1622 1623

- 1625 to Understand Reuse, Performance, and Hardware Cost of DNN Mappings. In *Proceedings of the 52nd IEEE/ACM International Symposium on Microarchitecture (MICRO)*. 1–14. <https://doi.org/10.1145/3352460.3358292>
- 1626 [40] Woosuk Kwon, Zhuohan Li, Siyuan Zhuang, Ying Sheng, Lianmin Zheng, 1627 Cody Hao Yu, Joseph E. Gonzalez, Hao Zhang, and Ion Stoica. 2023. Efficient 1628 Memory Management for Large Language Model Serving with PagedAttention. 1629 In *Proceedings of the 29th Symposium on Operating Systems Principles (SOSP)*. 1630 611–626. <https://doi.org/10.1145/3600006.3613165>
- 1631 [41] Chris Lattner, Mehdi Amini, Uday Bondhugula, Albert Cohen, Andy Davis, 1632 Jacques Pienaar, River Riddle, Tatiana Shpeisman, Nicolas Vasilache, and Oleksandr 1633 Zinenko. 2021. MLIR: Scaling Compiler Infrastructure for Domain Specific 1634 Computation. In *Proceedings of the IEEE/ACM International Symposium on Code 1635 Generation and Optimization (CGO)*. 2–14. <https://doi.org/10.1109/CGO51591.2021.9370308> Multi-level IR infrastructure enabling cost model composition 1636 across abstraction levels.
- 1637 [42] Hyojung Lee, Daehyeon Baek, Jimyoung Son, Jieun Choi, Kihyo Moon, and 1638 Minsung Jang. 2025. PAISE: PIM-Accelerated Inference Scheduling Engine for 1639 Transformer-based LLM. In *Proceedings of the IEEE International Symposium on High 1640 Performance Computer Architecture (HPCA)*. 1–14. PIM-based LLM 1641 inference scheduling. 48.3% speedup, 11.5% power reduction. Samsung..
- 1642 [43] Hayeon Lee, Seewoong Lee, Song Chong, and Sung Ju Hwang. 2021. HELP: 1643 Hardware-Adaptive Efficient Latency Prediction for NAS via Meta-Learning. 1644 In *Advances in Neural Information Processing Systems (NeurIPS)*, Vol. 34. 27016– 1645 27028.
- 1646 [44] Seunghyun Lee, Amar Phanishayee, and Divya Mahajan. 2025. NeuSight: GPU 1647 Performance Forecasting via Tile-Based Execution Analysis. In *Proceedings of the 1648 30th ACM International Conference on Architectural Support for Programming 1649 Languages and Operating Systems (ASPLOS)*. 1–15.
- 1650 [45] Jianbo Li et al. 2025. TrioSim: A Lightweight Simulator for Large-Scale DNN 1651 Workloads on Multi-GPU Systems. In *Proceedings of the 52nd Annual International 1652 Symposium on Computer Architecture (ISCA)*. 1–13. Multi-GPU DNN simulation 1653 with lightweight approach for distributed training analysis.
- 1654 [46] Shang Li, Zhiyuan Yang, Dhiraj Reddy, Ankur Srivastava, and Bruce Jacob. 2020. 1655 DRAMsim3: A Cycle-Accurate, Thermal-Capable DRAM Simulator. *IEEE Computer 1656 Architecture Letters* 19, 2 (2020), 106–109. <https://doi.org/10.1109/LCA.2020.2973991> Modernized DRAM simulator with thermal modeling and HMC 1657 support.
- 1658 [47] Wenzxuan Liang et al. 2025. Lumos: Efficient Performance Modeling and 1659 Estimation for Large-scale LLM Training. In *Proceedings of Machine Learning and 1660 Systems (MLSys)*. 1–16. Trace-driven performance modeling achieving 3.3% error 1661 on H100 GPUs for LLM training.
- 1662 [48] Haocong Luo, Yahya Can Tugrul, F. Nisa Bostancı, Ataberk Olgun, A. Giray 1663 Yağlıkçı, and Onur Mutlu. 2023. Ramulator 2.0: A Modern, Modular, and Extensible 1664 DRAM Simulator. *IEEE Computer Architecture Letters* 22, 2 (2023), 129–132. <https://doi.org/10.1109/LCA.2023.3333759> Modular DRAM simulator with DDR5, 1665 LPDDR5, HBM3, GDDR6 support and RowHammer mitigation modeling.
- 1666 [49] Peter Mattson, Christine Cheng, Cody Coleman, Greg Diamos, Paulius Micikevicius, David Patterson, Hanlin Tang, Gu-Yeon Wei, Peter Bailis, Victor Bittorf, 1667 et al. 2020. MLPerf Training Benchmark. In *Proceedings of Machine Learning and 1668 Systems (MLSys)*. 336–349. Standard ML training benchmark suite covering 1669 image classification, object detection, NLP, recommendation, reinforcement 1670 learning.
- 1671 [50] Azaz-Ur-Rehman Nasir, Samroz Ahmad Shoib, Muhammad Abdullah Hanif, and 1672 Muhammad Shafique. 2025. ESM: A Framework for Building Effective Surrogate 1673 Models for Hardware-Aware Neural Architecture Search. In *Proceedings of the 62nd 1674 ACM/IEEE Design Automation Conference (DAC)*. 1–6. 97.6% accuracy 1675 surrogate model framework for HW-aware NAS.
- 1676 [51] Amir Nasr-Esfahany et al. 2025. Concorde: Fast and Accurate CPU Performance 1677 Modeling with Compositional Analytical-ML Fusion. In *Proceedings of the 52nd 1678 Annual International Symposium on Computer Architecture (ISCA)*. 1–15. Hybrid 1679 analytical-ML approach achieving 2% CPI error at 5 orders of magnitude faster 1680 than gem5.
- 1681 [52] NVIDIA Corporation. 2019. Nsight Compute: Interactive Kernel Profiler. <https://developer.nvidia.com/nsight-compute>. Industry-standard GPU kernel profiling 1682 tool with roofline analysis.
- 1683 [53] Angshuman Parashar, Priyanka Raina, Yakun Sophia Shao, Yu-Hsin Chen, 1684 Victor A. Ying, Anurag Muber, Rangharajan Venkatesan, Brucek Khailany, 1685 Stephen W. Keckler, and Joel Emer. 2019. Timeloop: A Systematic Approach 1686 to DNN Accelerator Evaluation. In *Proceedings of the IEEE International Symposium 1687 on Performance Analysis of Systems and Software (ISPASS)*. 304–315. <https://doi.org/10.1109/ISPASS.2019.00042>
- 1688 [54] Jaehyun Park, Jaewan Choi, Kwanhee Kyung, Michael Jaemin Kim, Yongsuk 1689 Kwon, Nam Sung Kim, and Jung Ho Ahn. 2024. AttAcc! Unleashing the Power of 1690 PIM for Batched Transformer-based Generative Model Inference. In *Proceedings of 1691 the 29th ACM International Conference on Architectural Support for Programming 1692 Languages and Operating Systems (ASPLOS)*. 1–16. PIM-based accelerator for 1693 batched transformer attention. Seoul National University/UIUC..
- 1694 [55] Adam Paszke, Sam Gross, Francisco Massa, Adam Lerer, James Bradbury, Gregory 1695 Chanan, Trevor Killeen, Zeming Lin, Natalia Gimelshein, Luca Antiga, et al. 2019. PyTorch: An Imperative Style, High-Performance Deep Learning Library. In *Advances in Neural Information Processing Systems (NeurIPS)*, Vol. 32. 8024–8035.
- 1696 [56] Pratyush Patel, Esha Choukse, Chaojie Zhang, Aakanksha Shah, Íñigo Goiri, 1697 Saeed Maleki, and Ricardo Bianchini. 2024. Splitwise: Efficient Generative LLM 1698 Inference Using Phase Splitting. In *Proceedings of the 51st Annual International 1699 Symposium on Computer Architecture (ISCA)*. 118–132. <https://doi.org/10.1109/ISCA59077.2024.00019> Best Paper Award.
- 1700 [57] Hang Qi, Evan R. Sparks, and Ameet Talwalkar. 2017. Paleo: A Performance 1701 Model for Deep Neural Networks. In *Proceedings of the 5th International Conference 1702 on Learning Representations (ICLR)*. <https://openreview.net/forum?id=SyVVJ851g>
- 1703 [58] Aurick Qiao, Sang Keun Agrawal, Anand Jayaraman, Moustafa Mittal, Amar Altaf, 1704 Michael Cho, and Gennady Pekhimenko. 2021. Pollux: Co-adaptive Cluster 1705 Scheduling for Goodput-Optimized Deep Learning. In *Proceedings of the 15th USENIX Symposium on Operating Systems Design and Implementation (OSDI)*. 1706 1–18. Goodput estimation for co-optimizing resource allocation and training 1707 hyperparameters.
- 1708 [59] Jonathan Ragan-Kelley, Connally Barnes, Andrew Adams, Sylvain Paris, Frédéric 1709 Durand, and Saman Amarasinghe. 2013. Halide: A Language and Compiler 1710 for Optimizing Parallelism, Locality, and Recomputation in Image Processing 1711 Pipelines. In *Proceedings of the 34th ACM SIGPLAN Conference on Programming 1712 Language Design and Implementation (PLDI)*. 519–530. <https://doi.org/10.1145/2491956.2462176> Pioneerered separation of algorithm and schedule with learned 1713 cost models for autoscheduling.
- 1714 [60] Samyam Rajbhandari, Jeff Rasley, Olatunji Rber, and Yuxiong He. 2020. Zero: 1715 Memory Optimizations Toward Training Trillion Parameter Models. In *Proceedings 1716 of the International Conference on High Performance Computing, Networking, 1717 Storage and Analysis (SC)*. 1–16. <https://doi.org/10.1109/SC41405.2020.00024> DeepSpeed ZeRO optimizer partitioning for memory-efficient distributed training.
- 1718 [61] Mehdi Rakhshanfar and Aliakbar Zarandi. 2021. A Survey on Machine Learning- 1719 based Design Space Exploration for Processor Architectures. *Journal of Systems 1720 Architecture* 121 (2021), 102339. <https://doi.org/10.1016/j.sysarc.2021.102339>
- 1721 [62] Saeed Rashidi, Srinivas Srinivasan, Kazem Hamedani, and Tushar Krishna. 2020. ASTRA-SIM: Enabling SW/HW Co-Design Exploration for Distributed 1722 DL Training Platforms. In *Proceedings of the IEEE International Symposium 1723 on Performance Analysis of Systems and Software (ISPASS)*. 81–92. <https://doi.org/10.1109/ISPASS48437.2020.00018>
- 1724 [63] Vijay Janapa Reddi et al. 2025. MLPerf Power: Benchmarking the Energy Efficiency of Machine Learning Inference. In *Proceedings of the IEEE International 1725 Symposium on High Performance Computer Architecture (HPCA)*. 1–14. Energy 1726 efficiency benchmarking for ML inference workloads.
- 1727 [64] Vijay Janapa Reddi, Christine Cheng, David Kanter, Peter Mattson, Guenther Schmuelling, Carole-Jean Wu, Brian Anderson, Maxim Breeshkov, Mark Duber, et al. 2020. MLPerf Inference Benchmark. In *Proceedings of the 47th International 1728 Symposium on Computer Architecture (ISCA)*. 446–459. <https://doi.org/10.1109/ISCA45697.2020.00045> Standard ML inference benchmark suite with server and 1729 offline scenarios.
- 1730 [65] George F. Riley and Thomas R. Henderson. 2010. The ns-3 Network Simulator. 1731 *Modeling and Tools for Network Simulation* (2010), 15–34. https://doi.org/10.1007/978-3-642-12331-3_2
- 1732 [66] Arun F. Rodrigues, K. Scott Hemmert, Brian W. Barrett, Chad Kersey, Ron Oldfield, 1733 Marlo Weston, R. Risen, Jeanine Cook, Paul Rosenfeld, Elliott Cooper-Balis, and 1734 Bruce Jacob. 2012. The Structural Simulation Toolkit. In *ACM SIGMETRICS 1735 Performance Evaluation Review*, Vol. 38. 37–42. <https://doi.org/10.1145/1964218.1964225> Modular framework for system-level simulation, widely used for HPC 1736 and interconnect modeling.
- 1737 [67] Ananda Samajdar, Yuhao Zhu, Paul Whatmough, Matthew Mattina, and Tushar 1738 Krishna. 2019. A Systematic Methodology for Characterizing Scalability of 1739 DNN Accelerators using SCALE-Sim. In *Proceedings of the IEEE International 1740 Symposium on Performance Analysis of Systems and Software (ISPASS)*. 58–68. 1741 <https://doi.org/10.1109/ISPASS.2019.00016> Cycle-accurate systolic array simulator 1742 for DNN accelerator DSE.
- 1743 [68] Zhuomin Shen, Jaeho Kim, et al. 2025. AQUA: Network-Accelerated Memory 1744 Offloading for LLMs in Scale-Up GPU Domains. In *Proceedings of the 30th ACM 1745 International Conference on Architectural Support for Programming Languages and 1746 Operating Systems (ASPLOS)*. 1–16. <https://doi.org/10.1145/3676641.3715983> Improves LLM inference responsiveness by 20x through network-accelerated 1747 memory offloading.
- 1748 [69] Mohammad Shoeybi, Mostofa Patwary, Raul Puri, Patrick LeGresley, Jared Casper, 1749 and Bryan Catanzaro. 2020. Megatron-LM: Training Multi-Billion Parameter 1750 Language Models Using Model Parallelism. In *ArXiv preprint arXiv:1909.08053*. 1751 Intra-layer tensor parallelism for large language model training.
- 1752 [70] Srinivas Sridharan, Taekyung Heo, Jinwoo Choi, Garyfallia Yu, Saeed Rashidi, 1753 William Won, Zhaodong Meng, and Tushar Krishna. 2023. Chakra: Advancing 1754

- 1741 Performance Benchmarking and Co-design using Standardized Execution Traces.
arXiv preprint arXiv:2305.14516 (2023).
1742
- [71] Foteini Strati, Zhendong Zhang, George Manos, Ixeia Sanchez Periz, Qinghao
Hu, Tiancheng Chen, Berk Buzcu, Song Han, Pamela Delgado, and Ana Klimovic.
2025. Sailor: Automating Distributed Training over Dynamic, Heterogeneous,
and Geo-distributed Clusters. In *Proceedings of the 30th ACM Symposium on
Operating Systems Principles (SOSP)*. 1–18. Automated distributed training with
runtime/memory simulation over heterogeneous resources. ETH Zurich/MIT.
1743
- [72] Ondrej Sykora, Alexis Rucker, Charith Mendis, Rajkishore Barik,
Phitchaya Mangpo Phothilimthana, and Saman Amarasinghe. 2022. GRANITE:
A Graph Neural Network Model for Basic Block Throughput Estimation. In
*Proceedings of the IEEE International Symposium on Workload Characterization
(ISWC)*. 1–13. <https://doi.org/10.1109/ISWC55918.2022.00014>
1744
- [73] Vivienne Sze, Yu-Hsin Chen, Tien-Ju Yang, and Joel S. Emer. 2017. Efficient
Processing of Deep Neural Networks: A Tutorial and Survey. In *Proceedings
of the IEEE*, Vol. 105. 2295–2329. <https://doi.org/10.1109/JPROC.2017.2761740>
1745 Canonical DNN accelerator taxonomy covering dataflows, data reuse, and energy
efficiency.
1746
- [74] Philippe Tillet, H. T. Kung, and David Cox. 2019. Triton: An Intermediate Lan-
guage and Compiler for Tiled Neural Network Computations. In *Proceedings
of the 3rd ACM SIGPLAN International Workshop on Machine Learning and
Programming Languages (MAPL)*. 10–19. <https://doi.org/10.1145/3315508.3329973>
1747 Tile-based GPU programming with heuristic performance model for kernel
generation.
1748
- [75] Adrian Tschandl, Mohamed Awad, et al. 2025. SwizzlePerf: Hardware-Aware
LLMs for GPU Kernel Performance Optimization. arXiv preprint arXiv:2508.20258
(2025). LLM-based spatial optimization for GPU kernels, up to 2.06x speedup
via swizzling.
1749
- [76] Xizheng Wang, Qingxu Li, Yichi Xu, Gang Lu, Heyang Zhou, Sen Zhang, Yikai
Zhu, Yang Liu, Pengcheng Zhang, Kun Qian, et al. 2025. SimAI: Unifying Ar-
chitecture Design and Performance Tuning for Large-Scale LLM Training with
Scalability and Precision. In *Proceedings of the 22nd USENIX Symposium on
Networked Systems Design and Implementation (NSDI)*. 1–18. Full-stack LLM
training simulator achieving 98.1% alignment with real-world results. Alibaba
Cloud/Tsinghua..
1750
- [77] Zixian Wang et al. 2025. SynPerf: Synthesizing High-Performance GPU Kernels
via Pipeline Decomposition. arXiv preprint (2025). Under review.
1751
- [78] Samuel Williams, Andrew Waterman, and David Patterson. 2009. Roofline: An
Insightful Visual Performance Model for Multicore Architectures. *Commun.
ACM* 52, 4 (2009), 65–76. <https://doi.org/10.1145/1498765.1498785>
1752
- [79] William Won, Taekyung Heo, Saeed Rashidi, Saeed Talati, Srinivas Srinivasan,
and Tushar Krishna. 2023. ASTRA-sim2.0: Modeling Hierarchical Networks and
Disaggregated Systems for Large-Model Training at Scale. In *Proceedings of the
IEEE International Symposium on Performance Analysis of Systems and Software
(ISPASS)*. 283–294. <https://doi.org/10.1109/ISPASS57527.2023.00035>
1753
- [80] Yannan Nellis Wu, Joel Emer, and Vivienne Sze. 2022. Sparseloop: An Analytical
Approach to Sparse Tensor Accelerator Modeling. In *Proceedings of the 55th
IEEE/ACM International Symposium on Microarchitecture (MICRO)*. 1–15. <https://doi.org/10.1109/MICRO56248.2022.000078>
1754
- [81] Gyeong-In Yu, Joo Seong Jeong, Geon-Woo Kim, Soojeong Kim, and Byung-
Gon Chun. 2022. ORCA: A Distributed Serving System for Transformer-Based
Generative Models. In *Proceedings of the 16th USENIX Symposium on Operating
Systems Design and Implementation (OSDI)*. 521–538.
1755
- [82] Geoffrey X. Yu, Yubo Gao, Pavel Golber, and Asaf Cidon. 2021. Habitat: A
Runtime-Based Computational Performance Predictor for Deep Neural Network
Training. In *Proceedings of the USENIX Annual Technical Conference (ATC)*. 503–
521.
1756
- [83] Yi Zhai, Yu Cheng Wang, Peng Jiang, and Congming Kang. 2023. TLP: A Deep
Learning-based Cost Model for Tensor Program Tuning. In *Proceedings of the
28th ACM International Conference on Architectural Support for Programming
Languages and Operating Systems (ASPLOS)*. 833–845. <https://doi.org/10.1145/3575693.3575736>
1757
- [84] Li Lyra Zhang, Shihao Han, Jianyu Wei, Ningxin Zheng, Ting Cao, Yuqing Yang,
and Yunxin Liu. 2021. nn-Meter: Towards Accurate Latency Prediction of Deep-
Learning Model Inference on Diverse Edge Devices. In *Proceedings of the 19th
Annual International Conference on Mobile Systems, Applications, and Services
(MobiSys)*. 81–93. <https://doi.org/10.1145/3458864.3467882> Best Paper Award.
1758
- [85] Lianmin Zheng, Chengfan Jia, Minmin Sun, Zhao Wu, Cody Hao Yu, Ameer
Haj-Ali, Yida Wang, Jun Yang, Danyang Zhuo, Koushik Sen, Joseph E. Gonzalez,
and Ion Stoica. 2020. AnsoR: Generating High-Performance Tensor Programs
for Deep Learning. In *Proceedings of the 14th USENIX Symposium on Operating
Systems Design and Implementation (OSDI)*. 863–879.
1759
- [86] Lianmin Zheng, Ruochen Liu, Junru Shao, Tianqi Chen, Joseph E. Gonzalez,
Ion Stoica, and Zhihao Zhang. 2021. TenSet: A Large-scale Program Per-
formance Dataset for Learned Tensor Compilers. In *Advances in Neural Information
Processing Systems (NeurIPS)*, Vol. 34. 29876–29888.
1760
- [87] Yinmin Zhong, Shengyu Liu, Junda Chen, Jianyu Hu, Yibo Zhu, Xuanzhe Liu,
Xin Jin, and Hao Zhang. 2024. DistServe: Disaggregating Prefill and Decoding
1761
- for Goodput-optimized Large Language Model Serving. In *Proceedings of the 18th
USENIX Symposium on Operating Systems Design and Implementation (OSDI)*.
1762 1–18.
1763 1799
- 1800 1801
- 1801 1802
- 1802 1803
- 1803 1804
- 1804 1805
- 1805 1806
- 1806 1807
- 1807 1808
- 1808 1809
- 1809 1810
- 1810 1811
- 1811 1812
- 1812 1813
- 1813 1814
- 1814 1815
- 1815 1816
- 1816 1817
- 1817 1818
- 1818 1819
- 1819 1820
- 1820 1821
- 1821 1822
- 1822 1823
- 1823 1824
- 1824 1825
- 1825 1826
- 1826 1827
- 1827 1828
- 1828 1829
- 1829 1830
- 1830 1831
- 1831 1832
- 1832 1833
- 1833 1834
- 1834 1835
- 1835 1836
- 1836 1837
- 1837 1838
- 1838 1839
- 1839 1840
- 1840 1841
- 1841 1842
- 1842 1843
- 1843 1844
- 1844 1845
- 1845 1846
- 1846 1847
- 1847 1848
- 1848 1849
- 1849 1850
- 1850 1851
- 1851 1852
- 1852 1853
- 1853 1854
- 1854 1855
- 1855 1856